Quantitative measurement of aerosol deposition on skin, hair and clothing for dosimetric assessment. Final report

Fogh, Christian Lange; Byrne, M.A.; Andersson, Kasper Grann; Bell, K.F.; Roed, Jørn; Goddard, A.J.H.; Vollmair, D.V.; Hotchkiss, S.A.M.

Publication date:
1999

Document Version
Publisher's PDF, also known as Version of record

risø-r-1075(en)

Quantitative Measurement of Aerosol Deposition on Skin, Hair and Clothing for Dosimetric Assessment-Final Report

Fogh, C. L.; Byrne, M. A.*; Andersson, K. G.; Bell, K. F.*; Roed, J.; Goddard, A. J. H.*; Vollmair, D. V.*; Hotchkiss, S. A. M.*

*Imperial College of Science, Technology and Medicine,
T. H. Huxley School of Environment, Earth Science and Engineering.

Risø National Laboratory, Roskilde
June, 1999

Abstract In the past, very little thought has been given to the processes and implications of deposition of potentially hazardous aerosol directly onto humans. This state of unpreparedness is unsatisfactory and suitable protocols have been developed and validated for tracer experiments to investigate the deposition and subsequent fate of contaminant aerosol on skin, hair and clothing. The main technique applied involves the release and subsequent deposition on volunteers in test rooms of particles of different sizes labelled with neutron activatable rare earth tracers. Experiments indicate that the deposition velocity to skin increases linearly with the particle size. A wind tunnel experiment simulating outdoor conditions showed a dependence on skin deposition velocity of wind speed, indicating that outdoor deposition velocities may be great. Both *in vivo* and *in vitro* experiments were conducted, and the influence of various factors, such as surface type, air flow, heating and electrostatics were examined. The dynamics of particle removal from human skin were studied by fluorescence scanning. This technique was also applied to estimate the fraction of aerosol dust transferred to skin by contact with a contaminated surface. The various parameters determined were applied to establish a model for calculation of radiation doses received from deposition of airborne radioactive aerosol on human body surfaces. It was found that the gamma doses from deposition on skin may be expected to be of the same order of magnitude as the gamma doses received over the first year from contamination on outdoor surfaces. According to the calculations, beta doses from skin deposition to individuals in areas of Russia, where dry deposition of Chernobyl fallout led to very high levels of contamination, may have amounted to several Sievert and may thus be responsible for a significant cancer risk.

ISBN 87-550-2360-6
ISSN 0106-2840

Information Service Department, Risø, 1999

Contents

Preface

This report constitutes the final report for the EU project "quantitative measurement of aerosol deposition on skin, hair and clothing for dosimetric assessment" under the Nuclear Fission Safety RTD Programme, contract FI4PCT950019.

The project involves two partners: Imperial College from the UK and Risø National Laboratory from Denmark. The two partners have, for more than a decade, collaborated on indoor aerosol topics. The technique for labelling monodisperse particles with neutron activatable tracers was developed in close collaboration at the end of the 1980's for measuring indoor aerosol deposition velocities. Under the current contract the developed technique is being used to study the deposition to human body surfaces, such as skin, hair and clothing.

As a supplement to the original technique, Imperial College has developed a fluorescence scanning technique that has been used to study the particle-skin morphology and clearance from skin. Risø has made a dose model based on the parameters obtained during the project.

Both the partners in the project also participate in the EU Dermal Exposure Network (subgroups 4 and 5) dealing with surface contamination and source apportionment. Here the partners have gained useful knowledge from, for instance, dermatologists, and hope to disseminate the results to a wider forum.

This report is an expansion of the midterm report. Several tables and figures are identical to those in the previous report. Other tables and figures have been added or changed in order to take new data into account.

The support of NRPB in the UK for financing a PhD student at Imperial College is acknowledged. The work of this student provided complementary data for the current project.

1 Introduction

1.1 Objectives

A release of radioactive particles and gases from a nuclear installation will give rise to radiation exposure to workers and the surrounding population. In modelling of prospective accidents and dose reconstruction for past accidents, inhalation dose and dose due to external gamma radiation from the plume and from ground deposits are conventionally considered as the primary pathways at the time of the release. Deposits on skin of particles and reactive gases containing β-emitters will cause a dose to the skin and deposits on skin, hair and clothing will cause a γ-dose to the body. This contribution has so far largely been ignored in the estimates of total dose in accident consequence calculations, but in a recent article by the NRPB in EUR 13013 (Jones 1991) - The Importance of Deposition to Skin in Accident Consequence Assessments - calculations of the possible effect of a range of deposition velocities to the skin are presented. The paper states "The predicted expectation value of early deaths increases by about an order of magnitude over the range of deposition parameters considered here for a large accidental release." The paper contains a plea for experimental investigations into the processes of deposition to skin. Under an earlier contract the question of aerosol deposition to skin was addressed in a preliminary manner as part of a wider investigation concerning deposition of aerosol indoors. The initial measurements of deposition velocities to skin showed significantly higher values compared to those to passive surfaces such as walls of a room - this unexpected result has added to the importance of the present research. Thus previous work (including NRPB work) has highlighted three aspects of aerosol deposition to human surfaces: the radiological importance; unexpected high provisional deposition velocities and the complexity of the physics involved in the deposition and retention process. Particle retention by skin is a sampling issue in deposition and clearance studies. The kinetics of absorption and retention of a range of particles can be studied using animal and human skin in an in-vitro system currently established in the Imperial College Medical School. This in-vitro system has been shown to maintain the skin in a viable state and to provide an accurate and representative model of the in-vitro absorption of chemicals.

Drawing on previous developments in the generation of surrogate tracer aerosols, four research objectives have been identified in order to clarify the size and dosimetric effect of aerosol deposition on human body surfaces. These are:

1. Studying the physics of retention and sampling of particles from skin, hair, and clothing.
2. Measurement of deposition velocities to skin, hair and clothing, taking account of the wide range physical mechanisms (surface type, airflow, heating, electrostatics, etc.), and studying contaminant contact transfer to skin.
3. Estimating clearance rate of deposits from skin, hair and clothing: Natural clearance and forced clearance (e.g. decontamination)
4. Calculation of dose resulting from deposition at human body surfaces.

1.2 Work packages

Consistent with the important physics outlined in the objectives above, four work packages have been defined. The first three work packages deal with experimental work needed to establish the appropriate measurement protocols, understanding the processes and obtaining the relevant parameters for modelling. The last work package deals with the radiological modelling of the doses to man from aerosol deposition to the human body. For each work package a series of research tasks was defined and the subsection structure roughly follows the work tasks that was outlined in the work programme.

Sampling, together with retention on and clearance from skin is the topic of work package 1 (Chapter 2). Work package 2 deals with issues concerning clothing and hair (Chapter 3) and work package 3 deals with the deposition mechanisms (Chapter 4). In Chapter 5 the modelling of the dosimetric aspects of skin deposition is presented (work package 4).

1.3 Experimental techniques

The extensive collaborations between the partners in former projects has provided the ability to label, with sensitive stable (neutron activatable) tracers, aerosols from the sub-micron (from 0.1 microns upwards) to supra micron (from 20 microns downwards) sizes and to undertake clearance studies using fluorescent tracers. These experimental abilities are supported by the facilities available at both centres; aerosol laboratories, aerosol test chambers (capable of stimulating medium size rooms) test houses, wind tunnels and a nuclear reactor at each partner's establishment - to allow stable tracer neutron activation analysis (NAA).

The general experimental technique using neutron activatable tracers has been described thoroughly in several joint publications, including the production, dispersion and sampling of tracer aerosol. Byrne *et al*. (1995) describes test chamber procedures and Fogh *et al*. (1997) describes experiments in houses. Briefly, aerosols with a well-defined particle size are labelled with neutron activatable tracers that have a very low ambient concentration. These tracer particles are injected into rooms or test chambers and used to expose the objects of interest. Figure 1.1 shows the size distribution of three different tracers dispersed in an office experiment. It can be seen that the different tracers cover size ranges.

The particles larger than 1 μm are produced by labelling silica particles with Dysprosium or Indium. The silica is purchase at different nominal particle sizes: 1, 3, 5, and 20 μm. One batch of particles will be sufficient for a large number of experiments. For example, all experiment at Risø concerning the 1 and 5 μm nominal size particles have been performed with particles from the same batches. This ensures that the particle size is constant between experiments. An aerodynamic particle sizer, APS, and a Berner low-pressure impactor, BLIP, have been used to size the silica particles. In general, the silica particles are always referred to by the size obtained by the APS measurement as it is considered the most accurate. Table 1.1 shows a list of nominal and actual particle sizes.

The sub-micron particles is generated by nebulization of an indium acetylacetonate powder dispersed in alcohol. This generation method has the disadvantage that the particle size is not completely stable between different experiments. The aerodynamic diameter of the particles varied between 0.5 and 1.0

µm with a typical value of 0.7 µm. The size was measured with a Las-X optical instrument and a BLIP.

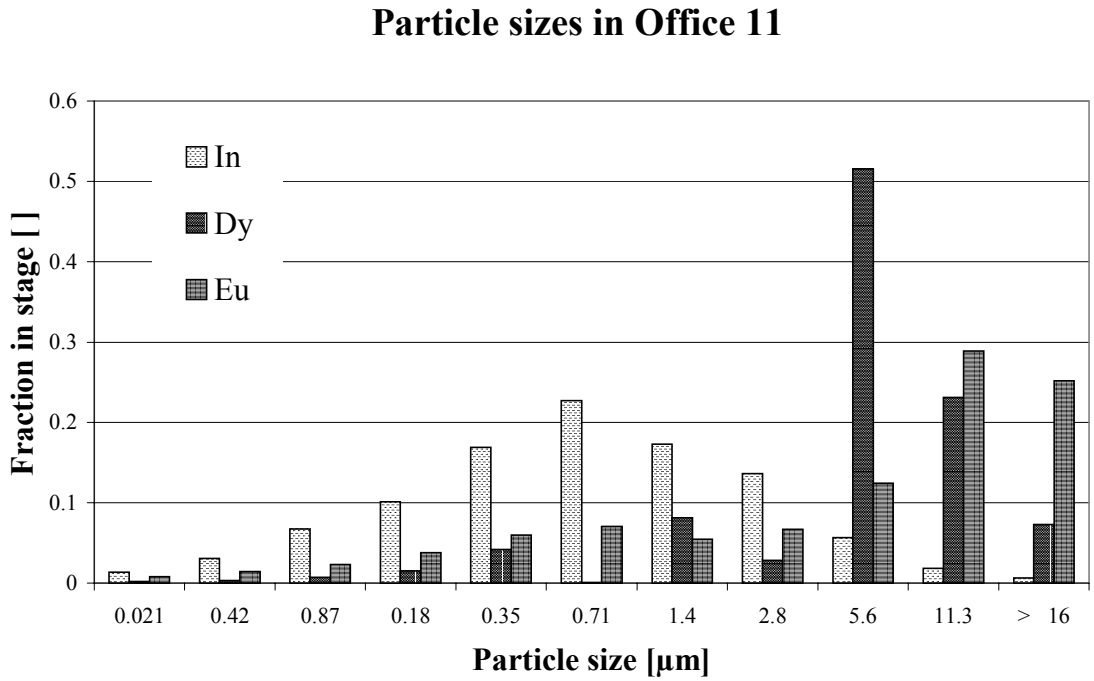

Figure 1.1 Size distribution of indium, dysprosium and europium during the 'Office 11' experiment measured with a Berner Low-Pressure impactor.

Table 1.1 Rewiev of particles and their sizes.

	Nominal size [µm]	Optical size measurement [µm]	BLPI size measurement [µm]
Indium acetyl-acetate	-	0.7	0.5 – 1.0
Silica with dysprosium	1	2.5	4.5
Silica with dysprosium	3	3	5
Silica with dysprosium	5	4.5	5.5
Silica with europeum	10	8.5	8.5

1.4 Definition and calculation of the deposition velocity

By measuring the air concentration by air sampling and the surface concentration on the objects the exposure can be expressed as a deposition velocity. The aerosol deposition velocity, v_d, to indoor objects has been defined by Roed and Cannell (1987) as:

$$v_d = F / C_0$$

where F is the flux to the surface and is measured as the mass per area divided by the exposure time and C_0 is the reference air concentration measured in the centre of the room or test chamber. The deposition velocity is the most

appropriate parameter for later modelling of the dose associated with exposure to a well defined release of particles.

In this project the objective is to measure deposition to human body surfaces such as skin, clothing and hair. Here the main experimental challenge is the retrieval of the deposited particles from the viable skin, whereas hair and cloth are simpler media as they can be bulk sampled.

The deposition velocities, v_d, presented in this section have been calculated from the following formula

$$v_d = \frac{Tracer\ mass\ deposited\ per\ area}{Average\ air\ conc.\ x\ Exposure\ time\ x\ Wiping\ efficiency}$$

where the tracer mass deposited is determined by bulk sampling or subsequent wiping, the average air concentration is determined by air filter sampling in the centre of the room or chamber, the exposure time is the residence time of the test persons in the test room. The wiping efficiency correction is taken from section 2.1 and is 0.73 and applied when wiping is used for sampling. When bulk samples, such as hair or cloth, is analysed the tracer recovery can be assumed to be 100 %.

2 Sampling, retention and clearance issues for skin

This integrated work package includes an investigation of: sampling procedures from skin, the clearance of particulate from skin, contact transfer to skin, and in-vitro studies of the mechanisms of particle retention by and penetration into skin.

2.1 Sampling of particulate from skin

An accurate knowledge of the removal efficiency and consistency of the skin sampling procedure adopted underpin the measured values of aerosol deposition velocity on skin (described in Chapter 4). A summary of dermal exposure assessment techniques is presented in Ness (1994). The principal techniques which can be applied to the measurement of tracer aerosol particles on skin are: (i) non-invasive optical scanning of the skin, exploiting fluorescent properties of the tracer particles, (ii) skin wiping, (iii) skin rinsing or washing, (iv) tape-stripping of the skin's upper layers, (v) using air-currents to resuspend or suck particles from skin, (vi) sampling surrogate surfaces attached to the skin. Only invasive skin sampling protocols were seen as appropriate for the current work; as will be discussed in detail below, the current state-of-the-art of optical scanning systems is that only relatively high tracer particle levels can be detected. This has implications for surrogate surface sampling also. The degree to which a surrogate surface is representative of skin can only be tested in comparison with a non-invasive contamination detection method such as skin scanning, since any other method (such as wiping, for example) used as a comparison, has its own inherent sampling uncertainties.

Several invasive skin sampling strategies were tested for particle removal efficiency and consistency; experiments, both in-vitro and in-vivo, are described below. The data generated in these tests have an additional relevance for the current work. Since invasive techniques remove particles from skin, informa-

tion on removal efficiencies, and on the fate of the remaining particles, can be used in the design of strategies for skin decontamination, following an accidental radioactive release to the atmosphere.

In-vivo experiments

As described in more detail in the section on test chamber experiments, 4.5 μm neutron activatable tracer labelled aerosol particles were injected into a test room which housed a human volunteer with exposed forearms. After 45 minutes, during which the aerosol was allowed to settle, the volunteer was removed from the test room, and strips of cosmetic hair-removing wax were then applied to the arms. Five exposures were carried out, and in each case, six wax strips were used. For comparison, other areas of the arms were wiped, with fabric wipes (60% cotton, 40% polyester, 2.5 cm^2), moistened with de-ionised water. No measure of the absolute deposition flux to the arms (which would require a non-invasive method) could be made in these measurements, so that it is not meaningful to quote a wiping or waxing efficiency. However, it could be seen that the coefficient of variation between samples was 28% in the case of waxing, and 21% in the case of wiping.

To determine quantitative skin wiping efficiency, the approach taken was to expose excised skin to neutron activatable particles, but then to fix this skin to a human volunteer during the wiping process. This would ensure that the skin was wiped with similar pressure to that exerted in wiping the human volunteers' own skin, and therefore, the study can be considered as, effectively, an in-vivo one. Sections of shaved rat skin were placed (on ice, to prolong viability) in an aerosol exposure chamber, and exposed to 4.5 μm particles for one hour. The skin sections were then halved and one side was fixed, exposed side upwards, to the back of the (gloved) hand of a human volunteer. The rat skin was then consecutively wiped with five fabric sections, which were moistened with de-ionised water. The wipes and the skin, both wiped and unwiped, were analysed, and particle removal efficiencies in the range 15-40% were recorded. The relative particle mass collected on the five wipes is shown in Figure 2.1, and it can be seen that particle recovery decreases with each subsequent wipe.

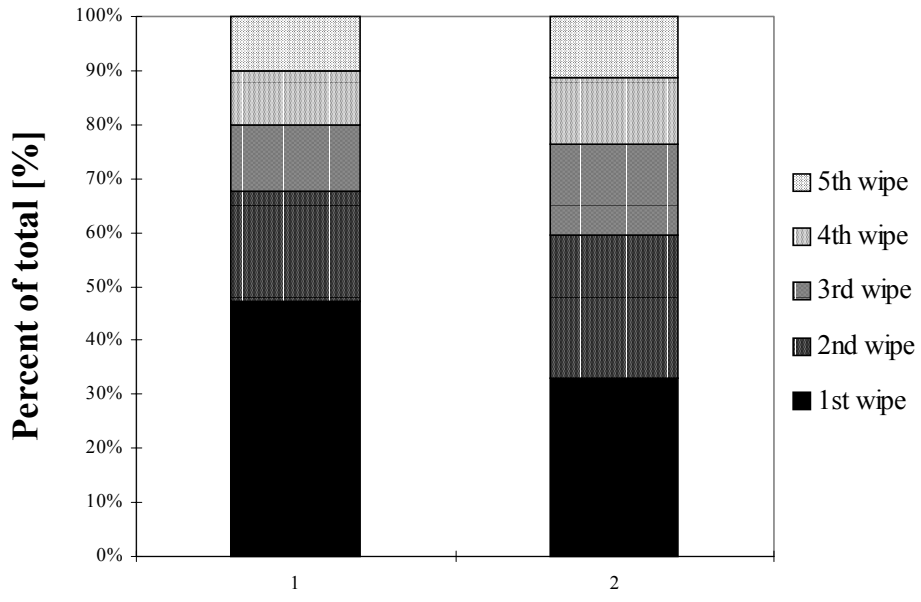

Figure 2.1 Histogram, showing the relative particle recovery on five consecutive wipes of skin exposed to 4.5 μm particles

A similar pattern can be seen for 0.5 and 2.5 μm particles in Figures 2.4 and 2.5 showing three consecutive wipes after an exposure in a house. However, analysis of the wiped skin itself indicated a significant quantity of residual tracer, suggesting that there exist a dislodgeable fraction, the distribution of which may or may not be modified by the wiping process. In Table 2.1 the relative distribution of recovered tracer by three subsequent wipes can be seen. The relative recovery of 0.5 μm particles by the first wipe (73 % of total) was higher than for 2.5 μm particles (66 % of total). This difference was significant ($p = 0.02$, $n = 37$).

Table 2.1 Tracer recovery on three subsequent wipes.

	No. sample locations	1st wipe [%]	2nd wipe [%]	3rd wipe [%]
0.5 μm particles	37	73 ± 15	17 ± 8	10 ± 9
2.5 μm particles	58	66 ± 17	21 ± 11	13 ± 11

In order to investigate the influence of the size of the sampled area on the amount of recovered tracer, areas of different sizes were wiped. In one experiment 8 cm^2 areas were wipe on the arms and 100 cm^2 areas were wiped on the chest and back of a volunteer. It was found that the amount of tracer per unit area was very similar for the two different area sizes: 18 ± 9 ng cm^{-2} versus 23 ± 13 ng cm^{-2} for the 0.5 μm particles and 5.5 ± 2.8 ng cm^{-2} versus 5.2 ± 2.8 ng cm^{-2} for 2.5 μm particles. As sufficient tracer could be detected on an 8 cm^2 area, it was decided to use this smaller area in future tests as this area could be better controlled with a metal template when wiping (as described in the sampling protocol in the Annex 9.1). Also, using a smaller area enables sampling to be carried out on a wider range of well-defined body parts.

Sampling efficiency

In order to determine quantitative tracer efficiencies, aerosol exposure of skin was carried out in a small (0.048 m^3) test chamber. The skin used in these experiments was hairless rat skin, chosen since it has a hair follicle density similar to human skin. The skin was cut into 1.7 cm diameter circles and throughout the aerosol exposure period, was kept viable by floatation on a physiological solution.

Quantitative sampling efficiencies were determined using skin exposed to neutron-activatable particles, and then subjected to the following particle sampling strategies: (i) an area of skin was wiped five times (ii) skin sections were pressed, exposed side down, on strips of cosmetic hair-removing wax, and then removed from the wax with tweezers (iii) skin samples were placed individually in jars filled with de-ionised water, and shaken vigorously for thirty seconds (iv) skin samples were subjected to a small vacuum-cleaning device, with a flow rate of approximately 15 litres min^{-1}, the nozzle of which was pressed against the sample surface for 10 seconds. It should be noted that the waxing and wiping procedures used were chosen to imitate those used in the in-vivo experiments, described earlier. The skin, wipes, wax, etc. were all analysed by NAA and Table 2.2. shows the mean removal efficiencies, with associated variation, of 2.5 , 4.5, 8 micron particles from skin (one hour exposure)

Table 2.2 Removal efficiencies for different sampling methods.

Particle Size [μm]	Wiping efficiency (%)	Waxing efficiency (%)	Washing efficiency (%)	Vacuuming efficiency (%)
2.5	72.5 +/- 8.8	75.8 +/-3.0	31.5 +/- 6.3	21.4 +/-3.5
4.5	71.1 +/- 8.1	77.0 +/-14.7	36.3 +/- 4.2	24.3 +/- 1.4
8	76.4 +/- 5.3	68.0 +/- 9.9	35.7 +/- 4.1	22.2 +/- 3.0

The effect of skin wiping on removal and redistribution of particles was studied using skin that had been exposed to fluorescent tracer labelled particles, for periods varying from 30 minutes to 5 hours. In this case, the skin sections, after particle sampling, were submerged in paraformaldehyde (to stop metabolic activity), dehydrated, embedded in paraffin wax, and then cut into 5 micron sections and examined under the fluorescent microscope. These results will be discussed in the section on particle retention below.

Based on the results shown in Table 2.2, washing and vacuuming were neglected as skin sampling strategies for the current work, due to their low efficiencies, and, in the case of washing, the anticipated difficulties in flowing liquid over a controlled area of skin. The wiping efficiency determined by using shaved rat-skin "in-vivo" was not considered to be reliable, due to the large number of hair follicles involved, relative to human skin; the merit of this experiment lies in the fact that it indicates that there is a dislodgeable fraction of particulate material on wiped skin, which is borne out in the in-vitro exposures of skin to fluorescent particles (discussed later). Although the in-vitro experiments, with hairless rat skin and neutron activatable particles, indicate that waxing and wiping had similar sampling efficiencies, it was observed that the variability associated with wiping is lower, and a similar observation was made in the in-vivo study. For these reasons, skin wiping was adopted as the preferred sampling strategy for the current work, and details of the wiping protocols are presented in Appendix 9.1.

2.2 Retention and clearance of particles from skin

For dosimetric assessment and decontamination, it is important to understand how particulate penetration, and removal efficiency, is influenced by the duration of skin exposure to the particles. As has already been indicated above, the skin has a unique surface and is therefore likely to exhibit very specific behaviour in terms of particle retention, which must be understood for radiological risk assessment. Studies aimed at understanding the time-course of particle removal from skin, both through active cleaning, and by the particles simply falling away during normal human activities are described below. Penetration of toxic particles below the skin's outer surface layer has the dual effect of exposing deeper layers of the skin and making the particles difficult to remove by any external means. The section on in-vitro studies describes experiments aimed at understanding the particle size dependence of dermal penetration rate, and also the influence of particle residence time on the skin. The relationship between skin wiping and skin penetration is also discussed in this section.

Fluorescence scanning system

In order to follow the time-course of particle removal from human skin, since that surface cannot be readily removed for analysis, it was necessary to develop a non-invasive analysis system. Fluorescence scanning has been applied to the

study of dermal contamination by several researchers, notably Fenske *et al.* (1996) and Roff (1994). The main components of their systems were an array of filtered lights, for illuminating a tracer aerosol, which had optimal fluorescence in a narrow wavelength range, and a filtered CCD camera, with image processing software, for collecting and analysing the fluorescence.

A review of the literature revealed that most earlier studies focused on the visualisation of highly fluorescent liquids under ultra-violet illumination. Design considerations for the present study took two factors into account. There are significantly smaller masses of tracer available in the present work, and the skin has an inherent fluorescence under ultra-violet illumination, which would be likely to interfere with the signal from the expected low particle concentration on the skin. Therefore, it was decided that a system would be developed which would rely on visible illumination. Fluorescein was the tracer chosen for the work, and the particles were dyed using a process described by Hodson et al (1994). The components of the fluorescence scanning system are described in detail in Annex 9.2.

Before it could be used in clearance studies, it was necessary to calibrate the fluorescence scanning system i.e. to determine the electronic signal associated with a known mass of tracer-labelled particles. The system was calibrated by suspending several samples of weighed tracer labelled silica in liquid water, and using a Buchner apparatus to evenly distribute the suspended material on filter papers. The dried filter papers where then analysed with the fluorescence scanning system, and a linear correlation ($R = 0.97$) between mass of tracer and fluorescent signal was obtained. An estimate of the limit of detection of the system was made: 2.5 mg of tracer particles cm^{-2}; this is significantly higher that the limit of detection of neutron activation analysis.

An important consideration in designing the fluorescence scanning experiments was ensuring that the tracer used did not degrade on exposure to sunlight or artificial light, thus giving the appearance of reduction in tracer concentrations on the skin. Prior to the experiments, tests were therefore carried out to ensure the stability of tracer-labelled particles on filter paper, when exposed for prolonged periods to sunlight outdoors, and also to electric light indoors.

Experiments were carried out, whereby 4.5 μm particles were applied to the forearms of volunteers by shaking the particles close to the skin and then removing the un-adhered fraction by gentle blowing. This approach was adopted since the limit of detection of the scanning system would have required that volunteers spent long periods in a test chamber if the arms were to be exposed by direct deposition. It was considered that localised application of tracer particles to the arms would represent a "worst case" scenario, from the point of view of clearance, since particle adhesion to the skin could not be lower, and might even by higher, than if deposition from ambient air had occurred. The level of loading of tracer particles on the skin was of the order of 40 mg cm^{-2}.

Approximately five minutes after exposure to particles, the volunteers' arms were rinsed with cold water. Tests were carried out on several different volunteers, with varying degrees of arm hair and the results showed that, in all cases, a single rinsing reduced the level of tracer on the arm to below the limit of detection (2.5 mg cm^{-2}). This indicates that the removal efficiency of cold water rinsing is greater than 90% for 4.5 μm particles. It should be noted that this value is considerably higher than the rinsing efficiency determined in the in-vitro studies presented in Table 2.1, where the particles resided on the skin for one hour before removal. It is also in contradiction to the hand wash results in the Office 9 - 16 tests, where a maximum of 50 % was removed after hand washing (see Chapter 4). The discrepancy between the values may indicate that

particle removal efficiency is a function of residence time on the skin; further evidence of this is presented in the next section.

Further studies were carried out whereby volunteers were exposed to 4.5 µm tracer particles, allowed to conduct their normal activities (ranging from sedentary indoor work, to outdoor walking) and were analysed at two-hour intervals. In each case, one of the volunteer's arms was treated with cosmetic moisturising cream (at a level thought to be representative of actual use), prior to particle loading. Figure 2.2 shows the pattern of clearance of particulate from the arms of two volunteers, one with little arm hair (MB) and one with significant arm hair (KB). The less hairy individual participated in some outdoor activity, in windy conditions, during the study period, while the hairier subject remained indoors. The results indicate that the residence of particles on the skin was influenced by the volunteer's arm hair concentration and the type of activity. This finding has important implications for persons unwittingly exposed to radioactive particles, and who do not take steps towards active decontamination. The use of moisturiser on the skin was not found to significantly influence particle retention: it was observed that moisturiser had the effect of retaining the particles only at the beginning of the test period, but this effect degraded quickly as the moisturiser was absorbed into the skin.

Further experiments were carried out to determine whether particle size was an important determinant of particle retention on skin. Using a single volunteer, particles of 4.5µm and 2.5µm diameter were applied to the forearm and hand (which had different degrees of hair cover) in separate tests; for each experiment, particles were applied to moisturised and unmoisturised areas of skin. Figure 2.3 shows a comparison of particle retention time on moisturised skin for the two particle sizes. The figure indicates that the efficiency of particle retention on skin increases by a discernible degree as particle size decreases: this is consistent with the results of indoor resuspension experiments (Thatcher and Layton, 1995).

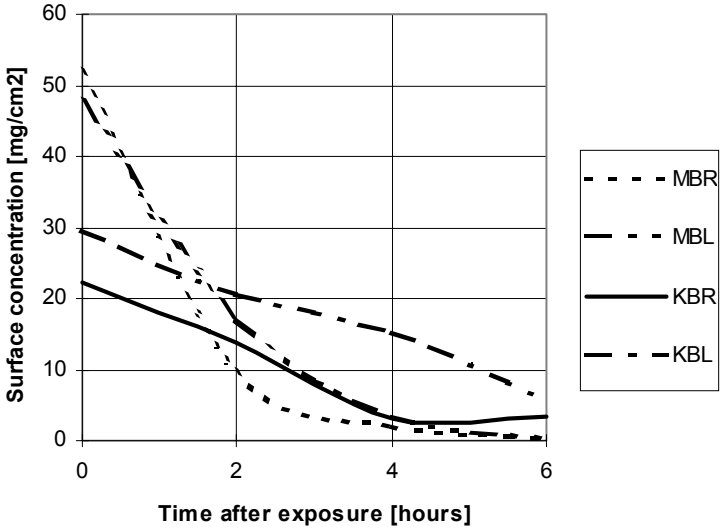

Figure 2.2. Curves showing the variation in particle loading on the arms with time, for two volunteers (MB and KB) on the right (R) and left (L) arm.

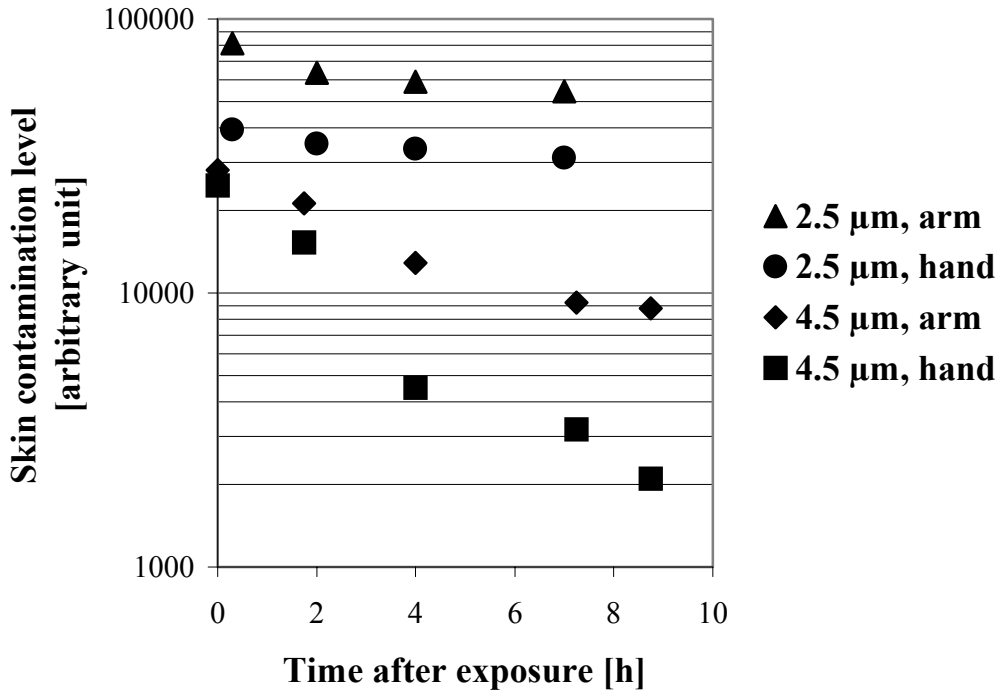

Figure 2.3 Curves showing the variation in particle loading with time on the forearms (hairy) and hands (minimal hair) of a volunteer, for two particle sizes: 2.5 µm and 4.5 µm

Two conclusions can be drawn based on the results shown in Figure 2.2 and 2.3: firstly, particles appear to fall off the skin more slowly with time, indicating the possible existence of a 'dislodgeable residue'. Secondly, the clearance half-life for the examined particle sizes is of the order of several hours, i.e. an appreciably shorter time than that used in accident consequence codes such as COSYMA- the model assumes a 30 day clearance half-life for particles from skin. This 30 day value is thought to be unrealistic, at least for these particle sizes – experiments carried out in the course of this work indicated that skin abrasion through contact with clothing while sleeping etc. had the effect of removing all detectable particles from the skin. In addition, it is known (Ness, 1994) that the body sheds its stratum corneum (skin's outer layer) in 2-3 weeks.

In-vitro studies.

Using an identical procedure to that described earlier in this section, hairless rat skin samples were prepared and exposed to fluorescent particles. Three particle sizes were used, with nominal aerodynamic diameters of 2.5 µm, 4.5 µm and 8 µm (these were the same particles which have been used for the deposition velocity measurements described in this report and elsewhere). The skin was exposed to each particle size for two time-periods: 30 minutes and 5 hours. In the final year of the work, post-operative human skin became available, and the experiments were repeated. In every case, the skin was collected from the operating theatre and used within one hour of the operation. The experimental procedures for exposure to particles and sample preparation were identical to those employed in the rat skin studies, although in the case of human skin, only two particle sizes, 2.5 µm and 4.5 µm, were used.

A selection of results is shown in Plates 1-6; Plates 1-3 are examples of rat skin exposure, and Plates 4-6 refer to human skin. The difference in the overall appearance of the plates arises because a dye is applied to the human skin prior to microscope slide preparation, but this is not the case with the rat skin. As can be seen in Plate 1, after 30 minutes, the 2.5 μm particles were distributed all over the stratum corneum and the hair follicles. Both the 4.5 μm particles and the 8 μm particles (not shown) were distributed over the stratum corneum, with the 4.5 μm, but not the 8 μm particles, exhibiting a tendency toward the hair follicles. As Plate 2 illustrates, after a five-hour exposure, the 2.5 μm particles had penetrated deeper into the hair follicles. The 4.5 μm particles (not shown) had penetrated to a lesser degree, and the 8 μm particles (not shown), while now tending towards the hair follicles, had not penetrated. These results indicate that particle size and residence time on the skin are both important determinants of particle penetrability, and hence, susceptibility for clearance; i.e. once the particles are below the skin surface their removal by external means becomes difficult.

Plate 3 shows wiped skin, which had had prior exposure to 2.5 μm particles for 5 hours. Comparison of this with Plate 2, which is a representation of a skin sample with an equal particle exposure time, indicates deeper penetration of the particles on the wiped skin, suggesting that the wiping process, although removing significant quantities of particles, may promote follicular penetration of particles. It may be concluded, therefore, that while wiping is an effective dermal exposure assessment technique, its effectiveness as a dermal decontamination strategy is compromised.

The conclusions from the experiments involving human skin were somewhat less clear than in the case of rat skin: it was difficult to conclusively determine a relationship between the degree of particle penetration and the exposure time and particle size involved. However, this was not necessarily considered to imply a difference in particle behaviour on human skin, but rather a result of human skin, relative to rat skin, having far fewer hair follicles, so that evidence of follicular penetration by particles was less obvious. Plate 4 shows that after 30 minutes' exposure, 2.5 μm particles were distributed indiscriminately across the surface of the human stratum corneum, with possible accumulation in the upper skin crevices/hair follicles, and occasional appearance of particles in the lower skin crevices and hair follicles. However, after 5 hours exposure (not shown) to 2.5 μm particles, no significant difference in appearance of the particles on the skin was observed. The 4.5 μm particles exhibited similar behaviour to the 2.5 μm particles for both exposure times; an example of a 5 hour human skin exposure to 4.5 μm particles is shown in Plate 5. As in the case of rat skin, wiping the human skin appeared to have the effect of enhancing the degree of particulate penetration into dislodgeable positions within the skin structure (Plate 6).

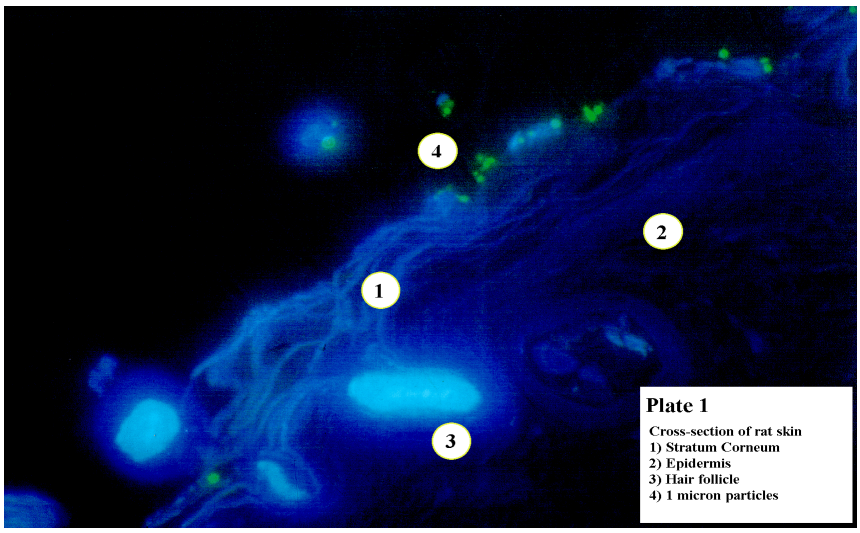

Plate 1 2.5 micron particles on skin for 30 minutes

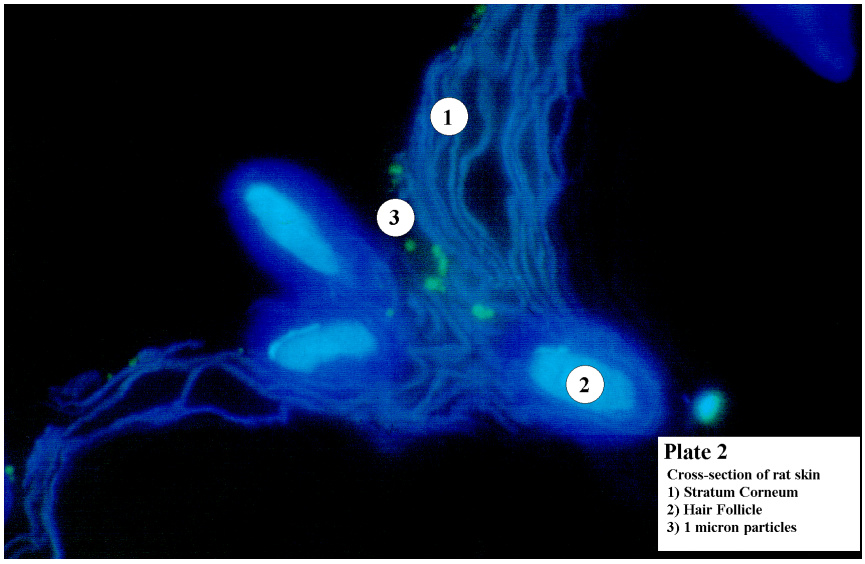

Plate 2 2.5 micron particles on skin for 5 hours

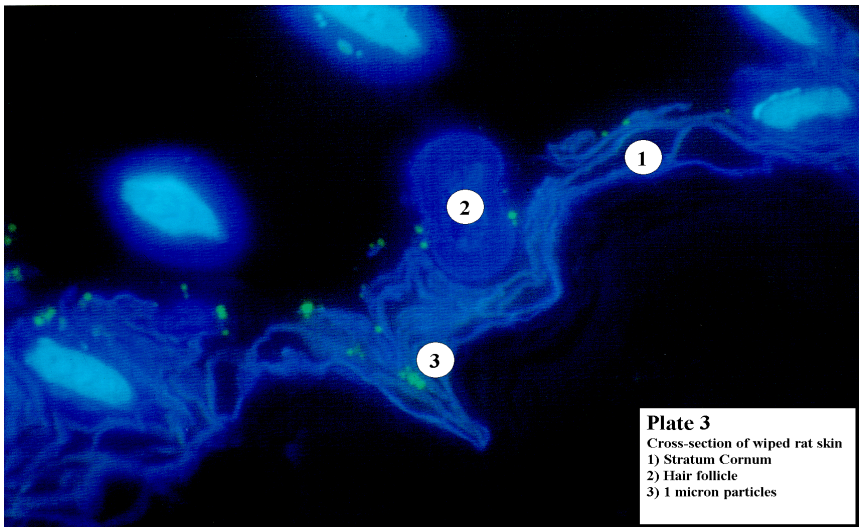

Plate 3 2.5 micron particles on skin for 5 hours, and skin then wiped

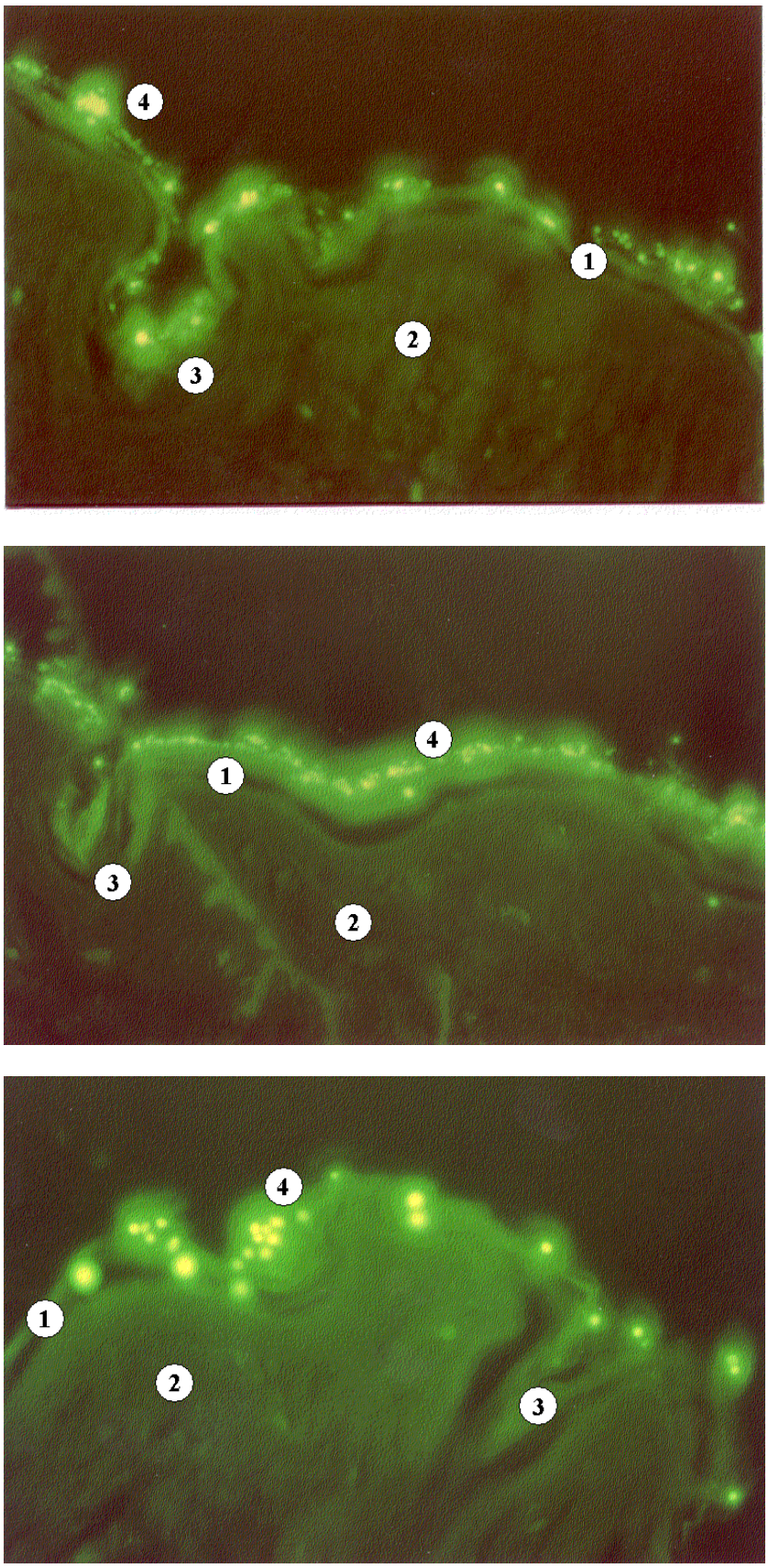

Plate 4 – 6 Cross-sections of human skin. (1) Stratum Corneum. (2) Epidermis. (3) Skin crevices or hair follicles. (4) Silica particles – top and middle are 2.5 micron particles, bottom plate is 4.5 micron particles.

2.3 Contact transfer

Preliminary experiments were designed to study the transfer of particulate contaminants from workplace and clothing surfaces to skin, in order to evaluate the contribution of this dermal contamination pathway to the total radioactive dose received by the body. In the occupational environment, contact transfer has already been extensively studied, but almost exclusively in the context of liquid contaminants. The most notable systematic study of contact transfer which concerns dry powders is that carried out by Brouwer *et al* (1999). Using fluorescent dyed particles, at loadings of 10-200 mg cm^{-2} on glass plates, they determined contact transfer efficiencies to volunteers' hands. To complement this study, the present work aimed to generate contact transfer data at lower surface loadings, to simulate the situation where a person might unwittingly become contaminated through contact with a surface which is not obviously contaminated.

The experimental strategy involved uniformly contaminating a test surface with neutron activatable particles, touching the surface with a gloved hand in a repeatable way, and then analysing the surface and the glove to determine the amount of transferred particles. Gloves were used because they could be analysed directly for tracer particles: this procedure eliminated concerns about uncertainties in particle recovery efficiency. The gloves chosen were made of textured latex, which was considered to be reasonably representative of the skin's surface.

The surfaces tested were smooth wooden board, polycotton fabric, synthetic knitted fabric, and polythene sheeting; these were intended to represent both clothing and workplace surfaces. The procedure used to deposit particles on the test surfaces was the same as that used to expose skin samples to particles in the in-vitro experiments (described earlier), i.e. by injecting particles from the RBG 1000 powder dispersion generator into a small aerosol exposure chamber, and allowing them to settle on a surface placed inside the chamber; preliminary investigations were carried out to ensure that the distribution of particles over the surface was uniform. The surface loading was determined by direct analysis of sections cut from the surfaces, except in the case of wood, where filter papers were placed on the wood and these were analysed instead. This was considered to be a valid strategy; the filter papers were similar in roughness to the wood, and as the surfaces were horizontally aligned, the primary aerosol dynamic process is gravitational settling (most of the tests involved 8 μm particles, although a small number were also carried out using 4.5 μm particles), which is not related to the surface type.

The experimental procedure was as follows: the test surface was exposed to tracer particles, and the gloved hand was then pressed down firmly onto the surface for 30 seconds. The same volunteer carried out all the experiments, so that the pressure used was relatively constant. Sections were then cut from the untouched part of the surface (except in the case of wood, when filter papers were used for sampling), and these were analysed together with the gloves. Experiments were carried out with dry and damp gloves.

The results of the experiments are shown in Table 2.3. The percentage contact transfer efficiency, C, is defined as

$$C = \frac{\text{Mass of tracer particle per unit glove area} \times 100}{\text{Mass of tracer particles per unit test surface area}}$$

	Cotton	Paper/wood	Jumper	Plastic
Dry gloves 10 µm	19.1 % (11.9%, 9)	20.8% (11.9%, 4)	21.5 % (11.4%, 5)	22.7% (11.1%, 9)
Dry gloves 5 µm	16.9% (5.2%, 12)	-	-	24.3% (11.4%, 6)
Damp gloves 10µm	30.5% (16.7%, 8)	30.2% (17.1%, 4)	28.5% (15.2%,4)	27.2% (15.0%, 6)

Table 2.3. Calculated contact transfer efficiencies. Standard deviations and no. of samples are shown in parentheses i.e. (standard deviation, number of samples) .

It can be seen from the results shown in Table 2.3 that an appreciable proportion of particulate material can be transferred to the skin through contact with contaminated surfaces. However, the variability associated with the results of these preliminary experiments is quite large in all cases, and it is therefore difficult to detect any dependency of contact transfer efficiency on particle size or on the texture of the contaminated surface. There is an indication, although not statistically significant, that damp gloves pick up more contaminant particles than dry gloves, which is not a surprising result. Further experiments are recommended to determine the surface and particle-related factors governing contact transfer efficiency.

2.4 Conclusions

The main achievement of work package 1 is the design and validation of the sampling protocol for particles on skin. This protocol is the basis for the retention and clearance experiments in work package one and the deposition experiments in work package 3. The protocol will also be useful in other fields of science, e.g. skin exposure assessments in occupational hygiene.

In the validation experiments in work package 1, human skin was used to investigate whether the wiping gave consistent results and rat skin was used to measure the actual wiping efficiencies. It was also established that using different wiping areas gave similar surface concentration results.

A fluorescence scanning system was developed and fluorescence microscopy was used to provide additional information on the impact of sampling on the distribution of deposited aerosol particles.

Clearance experiments carried out with the fluorescence scanning system suggested a clearance half life of particles from skin, which was lower than that generally accepted and more research is needed here.

3 Sampling, retention and clearance issues for clothing and hair.

In this chapter, dealing with work package 2, the issues of deposition to clothing and hair, together with retention and clearance from cloth and hair will be discussed.

The use of aerosol labels which can be analysed by neutron activation analysis, means that the highly sensitive analysis of deposition and retention on clothing and hair is straightforward as hair and most clothing materials have a low background when exposed to neutrons. Thus, samples cut from clothing and hair can be analysed readily using neutron activation analysis, by analysing bulk samples.

3.1 Deposition to clothing

In order to carry out deposition experiments a protocol for exposing and sampling the clothing is needed. The protocol for clothing sampling is simple, and is as follows:

1) A suitable air concentration of tracer particles is established in a room or test chamber as described in section 1.3. The particles will be of known size and the integrated air concentration is determined by air sampling.
2) The volunteer, wearing a selected clothing material, is exposed to tracer aerosol. The material should be test activated in a nuclear reactor beforehand to ensure that the background noise from trace elements in the cloth is sufficiently low to enable good detection of the tracer particles.
3) Using clean scissors, an unexposed individual wearing gloves cuts sections (approximately rectangular) from the clothing.
4) The position of the sample is measured, with respect to the shoulder of the garment in the case of a sleeve sample, and with respect to the neck of the garment in the case of a sample from the chest/back area.
5) The clothing sample is conveyed, with forceps, to a clean, labelled plastic bag.
6) The area of the sampled clothing is measured (samples are typically 10 to 20 cm^2).
7) The tracer content is determined by irradiating the entire sample in a nuclear reactor.

Using the protocol above, a series of clothing samples were obtained during test chamber experiments in the UK and under real life conditions in Denmark.

In Table 3.1 there is a review of the deposition velocities obtained during the first two years of the project. It is interesting to note that even though most of the samples were mounted in the vertical position on the chest and back of human volunteers, the deposition velocity is increasing with particle size, suggesting that inertial effects play an important role in the deposition process. The deposition velocities of 0.5 μm particles in the test chamber experiments were much higher than those found in the office and house environments, but it should be noted that a different kind of clothing fabric was involved. It can be seen that the roughly woven jumper having the largest surface area also had the highest deposition velocity and this is in good agreement with the expected behaviour.

Table 3.1 Review of deposition velocities obtained for clothing.

Experimental site	Type of Cloth	Number of samples	Deposition velocity [10^{-4} m s^{-1}] for particle size 0.5 µm	2.5 µm	4.5 µm
Office 6	Thick cotton	12	0.11±0.02	1.7±0.2	
Office 7	Thick cotton	12	0.91±0.52	4.5±1.3	
RH21	Thin cotton	6		4.4±0.4	
Test chamber	Jumper	12	22.0±1.2		35.0±1.3
Test chamber	Shirt	12	12.0±0.5		19.0±0.6

During the last year 10 different types of clothing material were exposed in order to investigate the hypotheses formed from the initial results: that rough surfaces would have higher deposition velocities than smooth cloth surfaces. The average deposition velocities for three samples after an exposure in the office 11 tests are presented in Table 3.2.

Table 3.2 Deposition velocity to 10 different types of clothing.

		Deposition velocity [10^{-4} m s^{-1}]		
Cloth description		**Particle size**		
ID	Composition, surface	0.5 µm	2.5 µm	8 µm
A	50 % viscose, 50 % acetose, very smooth	0.25 ±0.02	7.3 ±2.1	27 ±19
B	100 % wool, knitted – tight ribbed surface	0.56 ±0.08	17.6 ±1.0	129 ±51
C	100 % wool, knitted – very rough	1.17 ±0.60	10.2 ±3.8	BDL* -
D	100 % acrylic, knitted, ribbed– rougher than C	0.58 ±0.03	8.1 ±3.2	BDL* -
E	70 % cotton, 30 % polyester, smooth linen	0.29 ±0.07	14.1 ±3.3	100 ±72
F	65 % polyester, 35 % cotton, similar to A	0.33 ±0.01	10.5 ±3.6	42 ±30
G	65 % cotton, 35 % polyester, similar to E	0.69 ±0.06	16.4 ±1.2	145 ±20
H	50 % wool, 50 % acrylic, knitted ribbon – smoother than C	0.79 ±0.27	12.8 ±0.4	27 ±19
I	65 % cotton, 35 % polyester, similar to H	0.55 ±0.20	11.0 ±1.0	69 ±56
J	100 % cotton, smooth linen	0.23 ±0.05	8.6 ±0.0	66 ±17
	Average	0.55 ±0.29	11.6 3.5	76 ±45

* BDL: Below detection limit

The results presented in Table 3.2 have been also been presented in Figure 3.1. Here the samples are sorted according to increasing surface roughness from left to right. Especially for the small particles a clear dependency of surface roughness on aerosol deposition can be observed. All the ribbon knitted surfaces had higher deposition velocities than the smoother woven surfaces and the rough knitted material had the highest deposition velocity.

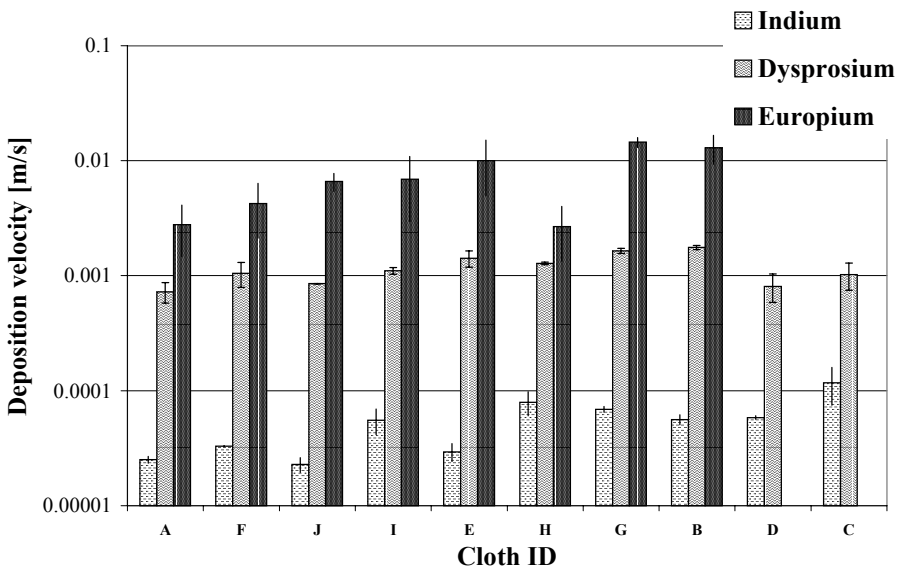

Figure 3.1 Deposition velocities for three particle sizes and ten different types of cloth. Each result is based on three samples. The samples have been sorted according to increasing roughness from left to right – A being smooth and C very highly textured.

3.2 Deposition to hair

Whereas analysis of hair is as straightforward as cloth sampling, some problems are associated with determining the projected area of a hair sample. Two different approaches have been used to solve this problem, as outlined below.

At Risø a sampling protocol for hair involving a complete hair cut has been utilised. The hair cut is performed in several stages, splitting the samples into inner and outer layers, so that an estimate of the depth profile of aerosol deposition can be made. The area of the test person's scalp is used as the deposition area. The major disadvantage of this approach is the long interval after sampling for which one most wait until the test person's hair will allow further sampling. Also, in the experiments carried out, no longhaired persons volunteered for a full hair cut.

The experience obtained from the full hair cut experiments was utilised to calculate deposition velocities based on smaller hair samples. The total weight of the hair from the full hair cut was 10 grams and as approximately two-thirds of the hair was removed it is estimated that the total mass of the test persons hair was 15 grams. The total area covered by hair was 0.09 m^2. During the office experiments described in Chapter 4, hair samples were taken at the root of the hair. The deposition per area was then determined by the following formula:

$$\frac{tracer\ per\ mass\ in\ sample * total\ mass\ of\ hair(15\ g)}{total\ area\ (0.09 m^2)}$$

This will give a rough estimate of the amount of tracer deposited per unit area.

At Imperial College, experiments have been carried out using full hair wigs, which are entirely sampled. After sampling the wigs are ashed before analysis. With this sampling strategy, sampling can be performed for as long as the wig supply continues. The major uncertainty in connection with the procedure is the question of whether the wigs, which are made of smooth nylon fibre, are repre-

sentative of human hair. Experiments have also been carried out at Imperial College whereby volunteers, while wearing swimming caps, were exposed to tracer particles; this was to simulate the case where an exposed person might have no head hair.

Table 3.3 presents the results of the hair deposition experiments. It can be seen that the deposition velocities for 2.5 and 8 μm particles are significantly higher than those presented in Table 3.1 for clothing. The deposition velocities to the swimming caps were at least as high as those to the wigs. This is unexpected as the wigs have a much larger surface area for deposition, but could be a plausible result if surface charge effects are considered as discussed in chapter 4. The result of the first full hair cut experiment was similar to that for wigs and caps for the larger particles, but a very high deposition velocity was found for the 0.5 μm particles. In the office experiments somewhat lower deposition velocities were found than those recorded for the full hair cut. They were, however, similar to those to the wigs.

Table 3.3 Deposition velocities to hair.

Deposition velocity 10^{-4} m s^{-1}	Particle size [μm] 0.5	2.5	8
Wig	25.0±1.2 (18)		34.0±1.1 (20)
Cap	26.0±2.1 (8)		53.0±4.8 (10)
Full hair cut	126 (1)	31 (1)	
Office 9 – 16	20±14(14)	14 (6)	

3.3 Clearance from clothing

Clothing contaminated with radioactive particulate may give rise to an external radiation dose to the wearer both initially and during subsequent re-wearing, if cleaning practices used were inefficient. The efficiency of particulate removal from clothing was investigated, using neutron-activatable tracers.

The decontamination effect of domestic washing procedures using washing machines has been studied in several experiments. Exposed pieces of cloth were cut into two pieces. One was washed and the pair was then activated so that the tracer contents could be compared. In Table 3.4 the results from three exposures can be seen. The Office 6 and 7 exposures occurred to two people wearing laboratory coats while sitting in an office, reading. 6 cloth pieces were sampled from each person and divided into two parts. The RH21 result was obtained by cutting samples from a T-shirt worn by a human volunteer in a room and the last two rows are for garments worn by test persons sitting in a test chamber. Generally, the smaller particles are more difficult to remove than the larger particles, suggesting that small particles will adhere better to the microstructures of the cloth, as can be seen in Table 3.4. The jumper was seen to be easier to clean than the cotton materials. Even though the curly macrostructure made the jumper have a higher aerosol deposition velocity than the cotton, the microstructure of the jumper was probably smoother as it was acrylic, thus explaining the lower adhesion of particles.

Table 3.4 Review of clearance from cloth of particles by domestic washing machines.

	Type of Cloth	Number of Pairs	Remaining fraction after wash for particle size		
			0.5 μm	2.5 μm	8 μm
Office 6	Thick cotton	12	0.80±0.22	0.60±0.12	
Office 7	Thick cotton	12	0.73±0.24	0.70±0.10	
RH21	Thin cotton	6	-	0.27±0.20	
Test Chamber	Jumper	12	0.31±0.07		0.11±0.02
Test chamber	Shirt	12	0.65±0.16		0.15±0.03

In order to test this assumption 10 new clothing types were exposed in a new test (Office 11) and washed in the same washing machine. The results are shown in Table 3.5. Here the washing efficiency was much higher. Nearly all contamination was here removed from the cloth and no differences could be observed between large and small particles or between different types of material (cotton, wool or acrylic).

Table 3.5 Clearance from 10 different kinds of cloth exposed during the Office 11 test and washed in a domestic washing machine.

Sample ID	Type of Cloth	Remaining fraction after wash for particle sizes	
		0.5 µm	2.5 µm
Cloth-A	50 % viscose, 50 % acetose	0.14	0.22
Cloth-B	100 % wool	0.10	0.03
Cloth-C	100 % wool	0.10	0.22
Cloth-D	100 % acrylic	0.00	0.20
Cloth-E	70 % cotton, 30 % polyester	0.12	0.51
Cloth-F	65 % polyester, 35 % cotton	0.30	0.72
Cloth-G	65 % cotton, 35 % polyester	0.36	0.16
Cloth-H	50 % wool, 50 % acrylic	0.11	0.10
Cloth-I	65 % cotton, 35 % polyester	0.07	0.00
Cloth-J	100 % cotton	0.11	0.14

In Figure 3.2 the combined clothing washing results from the Office 6 and 7 tests are presented together for the two different particle sizes, 0.5 and 2.5 µm. The amount of tracer after washing is presented as a function of the amount of tracer before washing on each sample. For both types of particles it seems that there is an approximately linear relation between the tracer amounts before and after washing, implying a constant decontamination factor, which is independent on particle loading and sample position. The fact that a regression line can be drawn with a zero intercept verifies that there is neither tracer background nor any non-removable fraction in the material tested. This is also true for the 10 types of clothing tested in Office 11.

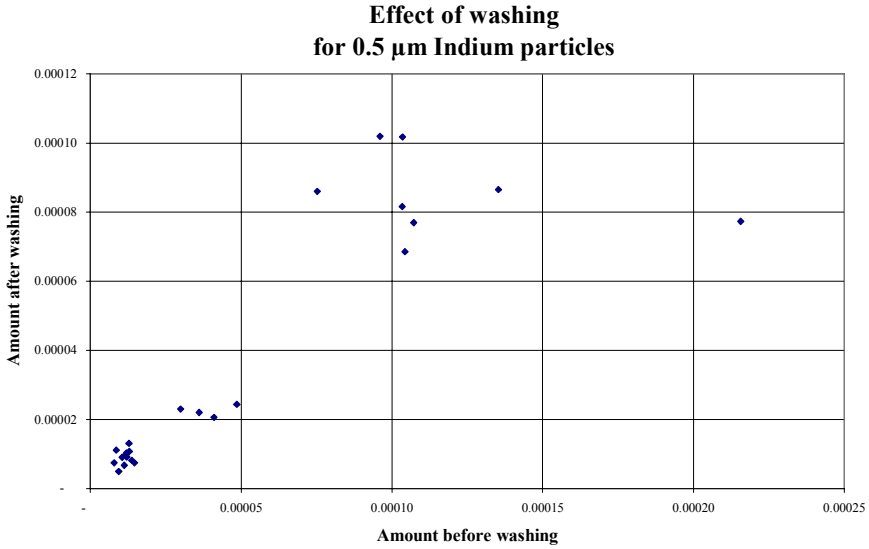

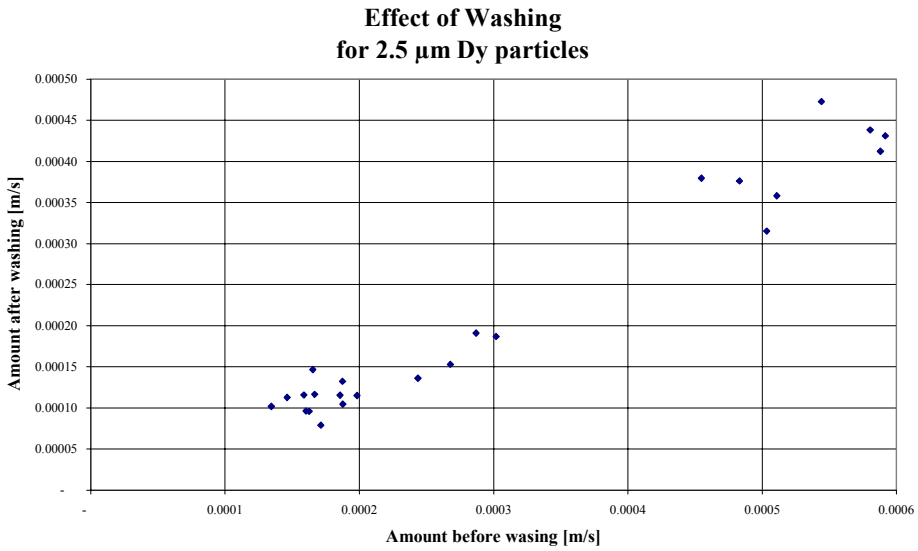

Figure 3.2 Effect of washing in a domestic washing machine at 40 °C for 0.5 µm particles (top figure) and 2.5 µm particles (bottom figure). Results are for laboratory coats made of cotton exposed in two different tests.

3.4 Clearance from hair

The clearance from hair can be studied by examining a time series of the tracer concentration in the hair samples. Figure 3.3 shows the results of experiments where test persons were exposed to tracer particles two times each day (office tests 9 - 16). Each point is based on two samples. It can be seen that the pre-samples taken in the morning show a stable background value of indium, representing the 0.5 µm particles. As a background content of tracer would be homogeneously distributed in the hair, this result is expected. After each exposure a marked increase in the tracer concentration can be seen. These values have greater deviations, due to the fact that it is difficult to collect samples of hair on each occasion that have been equally exposed. It should be noted that the emission system in the Office 12 experiment failed so there should be no additional exposure in that case: the results verify this.

The test person had a shower each morning including a hair wash. This was obviously sufficient to remove the tracer aerosol to which he had been exposed in the previous day's tests. However, it is possible that other types of aerosol, which were not investigated in this work, might show greater adherence. It is, however, expected that larger particles will be bound less strongly.

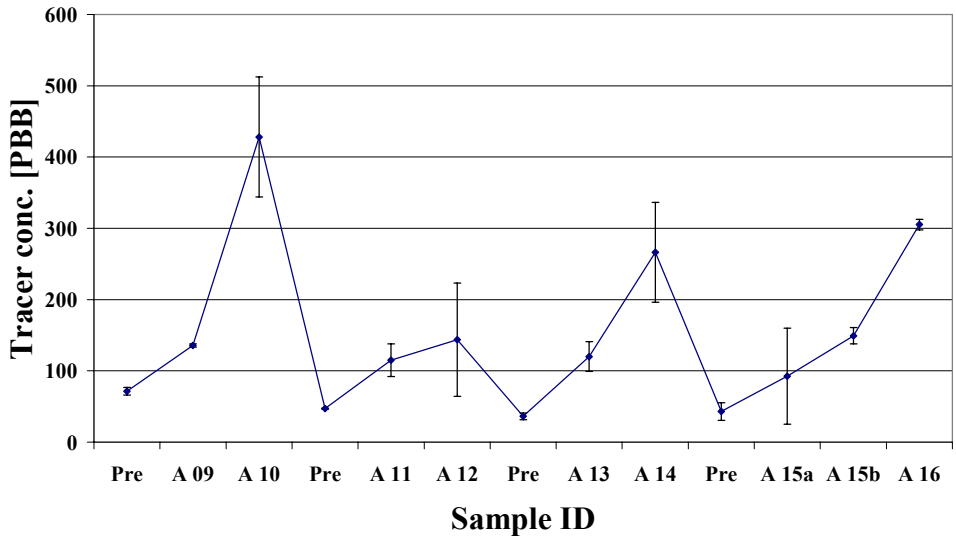

Figure 3.3 Indium tracer concentration (0.5 µm) in hair samples before and after the 8 office experiments, Office 9 – 16, at Risø, June 1998.

4 Aerosol deposition velocity to skin

Deposition velocities to human surfaces have been investigated in two stages; firstly in test chambers, and, secondly, in realistic indoor environments (e.g. persons in rooms where, for example, electrostatic effects from the use of computers may be important). Factors relevant to the outdoor environment have also been considered. Results from the sampling and retention research described in section 2.1 above are utilised. The following have been investigated for a range of particle sizes: air-flow-conditions (including the effect of the body heat island, environmental flow-generated turbulence and body movement), electrostatic fields and the variability of the human body surfaces in question.

4.1 Test chamber measurements.

Extensive measurements of aerosol deposition on the body, under simulated indoor conditions, have been carried out using a 32 m^3 test chamber. The experimental procedure essentially involved a human volunteer(s) entering the test chamber after tracer aerosol had been released and well-mixed by other personnel, and remaining there for up to 45 minutes. Aerosol concentration measurements were made via a dichotomous aerosol filtration system at the centre of the test room. A small fan was used throughout the aerosol mixing period, and remained running during the deposition interval, but care was taken to ensure that the volunteer was not seated in the direct path of the fan, and that impaction of particles carried by the fan did not significantly contribute to the flux to the body.

In most cases, the volunteer remained seated in the chamber throughout the experiment, and the only movement was that necessary to change the air filters. Following the aerosol deposition period, the volunteer left the test chamber and

wipe samples were taken from the forearms, and in some cases, from the face, as described in section 2.1.

Using three aerosol particle size distributions, 2.5, 4.5, and 8 μm, in excess of 50 individual volunteer exposure events were carried out, resulting in 176 skin wipe samples. Table 2.5 presents the measured aerosol deposition velocities, averaged over all samples. Statistical analyses were carried out to ascertain whether there was a significant difference between deposition velocities to the arm and face of the individual volunteers; no difference was found. Neither was there a significant difference in deposition velocity to the arms of different volunteers (who had different levels of arm hair).

Table 4.1 Measured aerosol deposition velocities to skin; data (means and standard deviations) derived from experiments involving three human volunteers.

Particle size	2.5 μm	4.5 μm	8 μm
Deposition velocity [10^{-4} m s^{-1}]	9.9-16.1	71.2-128.8	107.9-192.1
No. of samples	20	114	42

In several of the tests, filter papers were attached to the walls and floors of the test chamber throughout the deposition period. These yielded the result that, for 4.5 μm particles, the average deposition velocities to the vertical and horizontal surfaces of the test chamber were of the order of 10^{-5} m s^{-1} and 10^{-4} m s^{-1}, respectively. As can be seen from Table 4.1, relative to these values, aerosol deposition velocities to the skin were found to be high. It was therefore considered to be of interest to examine the influence on deposition velocity of some of the individual factors characterising the human body: electrostatics, heat, and surface roughness.

Determination of aerosol deposition velocities by skin wiping, as described earlier, incorporates issues of deposition on surfaces of different roughness, but also issues of retention of material to a different degree when these surfaces are wiped. As stated earlier, no significant difference was observed between aerosol deposition velocities on hairy and non- hairy volunteers, which may indicate that enhanced deposition promoted by increased roughness may be concealed by difficulty in removing aerosol from rougher surfaces. Alternatively, it may indicate that another skin-related factor is more significant than roughness. For this reason, in order to fully understand the dependence of aerosol deposition velocity on surface roughness, it is instructive to measure direct deposition on surfaces of varying roughness' attached to the skin. This was achieved by attaching small squares (typically 12 cm^2) of felt, plastic and polythene to the forearms of the volunteer by means of adhesive spray. The volunteer was then exposed to aerosol as previously described, and the samples were removed for analysis after an appropriate deposition period. In some cases, a heated aluminium cylinder 1.5 m high and 0.15 m diameter, to which felt, polythene and filter paper samples were attached, was also present in the test chamber. The cylinder had the advantage of a greater surface area, relative to the human arm, on which to mount samples, so that possible differences in aerosol deposition due to spatial variability could be averaged out in a large number of samples. Also, the cylinder was completely immobile so that any effects due to aerosol deposition via impaction on samples attached to the human body could be eliminated.

Aerosol deposition velocity measurements were made with three particle size distributions: 2.5, 4.5 and 8 μm; the cylinder was only present in the test chamber for those experiments involving 2.5 and 8 μm particles. The data are shown in Table 4.2. Statistical tests showed that there was no significant difference

between aerosol deposition to samples attached to the arm and to the cylinder, and data derived from both bodies are therefore shown together in Table 4.1. It can be seen that while aerosol deposition to felt is greater than to smoother filter paper, the greatest deposition velocity was observed to the smoothest surface: polythene. However, statistical analysis showed that the difference between deposition on felt and plastic is not significant at the 95% confidence interval for 8 μm particles. This indicates that another factor associated with plastic surfaces- electrostatic charge- is an important modifier of aerosol deposition.

Table 4.2 Cylinder experiments. Deposition velocities for three different surface types mounted on a cylinder. The 95% confidence intervals are quoted with the number of tests in parenthesis.

Deposition to surface types	Particle size [μm] 2.5	4.5	8
Filter paper [10^{-4} m s^{-1}]	1.0-1.4 (16)	5.4-8.6 (8)	10-25 (18)
Felt [10^{-4} m s^{-1}]	2.0-4.6 (16)	14-26 (33)	25-49 (18)
Polythene [10^{-4} m s^{-1}]	2.8-8.4 (16)	12-48 (39)	22-61 (18)

Electrostatic charge may be generated by tribo-electrification of both footwear and clothing (Greason 1994) and is held by the insulating qualities of the clothing and skin (Grandolfo *et al.*, 1985). Aerosol transport theory suggests that electrostatic charge influences aerosol deposition, particularly for the smaller particle sizes, but the relevance of this information for the present work is unclear since little quantitative data are available on charges on the human body. It is known, however, that electrostatic charge on the body is highly variable. No attempt was made in the current work to improve this, but experiments were simply carried out to determine the difference in aerosol deposition velocity to skin, which was held at electrical ground potential, and skin which was at "normal" potential. An elastic electrical conducting strap, of the type used by computer repair personnel, was attached to one wrist of a volunteer, and the other end of the strap was connected to the wall of the laboratory. As before, the volunteer was exposed to tracer aerosol (4.5 μm particles) and both the grounded and ungrounded arms were then wiped. The experiment was repeated six times, with the conducting strap alternated between the volunteer's arms. The result is shown in Table 4.3.

Table 4.3 Review of experiments testing electrostatic effects on the deposition process for 4.5 μm particles.

	Grounded arm	"Normal" arm
Deposition velocity [10^{-4} m s^{-1}]	59.0	99.0
Standard deviation [10^{-4} m s^{-1}]	8.5	20.8
No. of samples	18	18

Another mechanism suspected to be responsible for the high magnitude of aerosol deposition (relative to internal building surfaces) on body surfaces was convection caused by the heat of the human body. Using neutron-activatable tracers and the heated aluminium cylinder as in the present work, it was observed by Bell (1994) that heating the cylinder to human body temperature resulted in enhanced aerosol deposition on the cylinder's surface. Nazaroff and Cass(1987) postulated that when a flat vertical plate is heated, particle deposition is likely to be enhanced when the characteristic surface roughness is less than the concentration boundary layer caused by thermophoresis. It was calcu-

lated that for a particle diameter of 3 μm and an air-surface temperature difference of 10K, the concentration boundary layer close to a surface is of the order of 0.5 mm, significantly less than the likely roughness height of the human body. Enhanced aerosol deposition on the human body cannot therefore be easily explained by thermophoresis, but is more likely to be attributable to turbulence generated by convective currents. Fluctuations in aerosol concentration due to turbulence in proximity to heated human phantoms have been reported by Parker *et al.* (1990).

In the present work, it was not possible to measure aerosol concentration fluctuations close to the body of a human volunteer, but measurements of air velocity with distance from the body were made, using hot- wire anemometers. It was found that the maximum air velocity occurred near the chest of the volunteer, and was 0.25 m s^{-1}, falling to 90% of this value at a distance of 20 mm. This finding is in good agreement with the observations of Homma and Yakayima (1988), who used infra-red thermography to visualise the thermal envelope around the body.

4.2 Realistic environments

Aerosol deposition experiments involving human volunteers have been carried out at Risø in office environments and under domestic conditions. Until now 16 exposures have been carried out in office environments and three in houses. The results of the first two office experiments and one house experiment were presented in the report of an earlier EU contract.

Results from the first two years

During the first two years 4 experiments in offices and two in residential houses were carried out.

In each office experiment the same two male test persons were exposed. The persons entered the office after a well mixed tracer concentration was established and a third person in the test room carried out the particle dispersion, air sampling, wind velocity measurements, etc. A fourth unexposed person performed the skin wiping in a neighbouring room after the test. The length of the exposure was varied in order to allow plotting of the recovered amount of tracer as a function of the integrated air concentration. In order to permit detailed examination of the variability of the data it was decided to focus on only two particle sizes: 0.5 μm indium particles and 2.5 μm dysprosium particles. In two of the tests (Office 4 and 5) one of the test persons was working by a PC (KGA) and the other person (CLF) was reading. In the two other tests (Office 6 and 7) both test persons were reading. Office 8 was a joint experiment between Imperial College and Risø and it was carried out for the purpose of comparison of the experimental procedures used by the partners.

In Table 4.4 the deposition velocities found in the six different tests are presented. For the four office experiments, results for the two test persons are presented individually, and as an overall average. It can be seen that the results for KGA were similar regardless of whether or not he was sitting in front of a PC. For the 0.5 μm particles there was a slight increase in deposition velocity from 0.00023 to 0.00034 m s^{-1}, but this was not significant ($p = 0.15$ in a t-test). For the 2.5 μm particles there was no difference in the overall mean deposition velocity: 0.0040 versus 0.0040 m s^{-1}.

When the deposits to the two different test persons were compared it was found that the deposition velocity was significantly higher to KGA than to CLF. For the 0.5 μm particles the deposition velocity increased from 0.00013

for CLF to 0.00019 m s^{-1} for KGA and this increase of 46 % was significant (p=0.004). For the 2.5 μm particles the increase was 112 % from 0.0019 m s^{-1} for CLF to 0.0040 m s^{-1} for KGA and this increase was also significant (p=0.003). The most evident difference between the two test persons is that CLF has limited arm hair growth whereas KGA has rather hairy arms. This result has also been observed in previous experiments reported by Lange (1995), but the results obtained in the test chamber experiments indicated that arm hair concentration was not an important determinant of aerosol deposition velocity.

Table 4.4 Average deposition velocities for different persons in different tests.

	Number of sample locations [ ]	Particle size 0.5 μm [10^{-4} m s^{-1}]	2.5 μm [10^{-4} m s^{-1}]
CLF	5	2.0±3.3	7.5±3.8
KGA (PC)	5	4.6±2.7	40.8±35.4
Office 4 average	**10**	**4.0±2.3**	**24.1±29.6**
CLF	5	0.8±0.3	16.3±5.6
KGA (PC)	5	2.3±0.9	38.6±15.4
Office 5 average	**10**	**1.5±1.0**	**27.5±16.0**
CLF	5	0.6±0.2	18.7±5.8
KGA	5	2.9±1.6	45.5±23.1
Office 6 average	**10**	**1.7±1.6**	**32.1±21.2**
CLF	5	0.4±0.2	32.6±8.8
KGA	5	1.8±1.9	34.2±24.3
Office 7 average	**10**	**1.1±1.5**	**33.4±17.3**
RH39 average	17	1.1±0.6	27.5±14.3
RH21 average	21	NA	19.6±19.8

In Figure 4.1 the results from the Office 6 test are shown for the indium particle used. It can be seen that the deposition velocity is higher for the KGA test person (prefix 'K' to the right in the figures than to the test person CLF (prefix 'C' to the left on the figures). When compared with the dysprosium deposition pattern (see midterm report, Roed *et al*. 1998) it can also be seen that the deposition patterns for the two different particle sizes are similar: the minimum and maximum deposition velocities occurs at the same sampling locations. As discussed in section 2.1 the figures also illustrate that most of the tracer is removed with the first skin wipe and the tracer level thereafter decreases with subsequent wipes. Figure 4.1 also demonstrates that there is a difference between upwards and downwards facing wiping locations on the arm. The suffix 'U' means under (or downwards) and the suffix 'O' means over (or upwards) and it can be seen that there is a higher deposition to the upwards facing location. This pattern was observed in most of the tests.

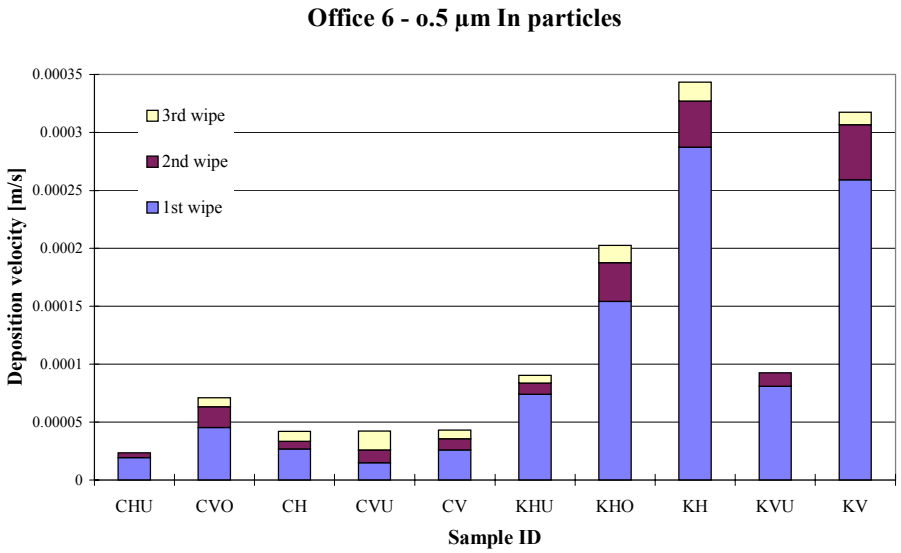

Figure 4.1 Deposition velocities for 0.5 µm indium particles obtained by three sequential skin wipes on five locations on two different test-persons (CLF is prefix 'C' to the left and KGA is prefix 'K' to the right).

In the two experiments in real houses (denoted RH39 and RH21), 5 different persons were exposed (a total of 10 different persons for the two tests), that had not previously participated in the skin wipe experiments. This was done in order to increase the sampling population. As can be seen in Table 4.3 the average deposition velocities found in the two house experiments were close to those determined in the office experiments.

Experiments in 1998

In June 1998 an additional 8 experiments in offices were carried out at Risø (office 9 – 16). The measurements were carried out in close collaboration between Riso and Imperial College.

A number of parameters were systematically varied between the tests and a large number of samples were exposed and collected. In Chapter 3 the results of the clothing and hair exposures were reported.

In addition to the indium and dysprosium tracers that were used in the previous tests, silica particles labelled with europium were also used in this test. In this way deposition of three different particle sizes could be investigated in the same experiment. The europium mass load in the air was, however, not as elevated as was the case for the two other tracers and the uncertainty on the europium results is significant. The three independent particle size distributions are illustrated in Figure 1.1.

Figure 4.2 shows the results from the Office 11 test. As in the previous test series three sequential skin wipes were carried out. All together this resulted in twelve wipes per test person in each test. Similarly to the results for indium in the earlier experiments shown in Figure 4.1 the first wipe removed the most tracer. The second wipe removed less tracer than the first and the third wipe removed the least tracer.

In this series of tests, the effect of hand washing on tracer particle removal was examined. In tests 9, 11, 13 and 15, following exposure, the right hand and arm were wiped first, after which the test person washed his/her hands with soap and water. The left hand and arm were then wiped. In Office 10, 12, 14 and 16 the procedure was mirrored so that the left arm was wiped first in order to eliminate any differences between washing efficiencies amongst the two

sides. In Figure 4.2, which shows results from test 11, this effect can be seen as a lower deposition velocity to the left arm. Table 4.5 summarises the recorded washing efficiencies. The washing efficiencies obtained for the dysprosium and europium labelled silica particles, 2.5 and 10 µm, are in good agreement with the results from the test chamber experiments presented in Table 2.2. The smaller indium particles, 0.5 µm, were found to have a lower washing efficiency, which suggests that the wiping efficiency is also lower for these particles.

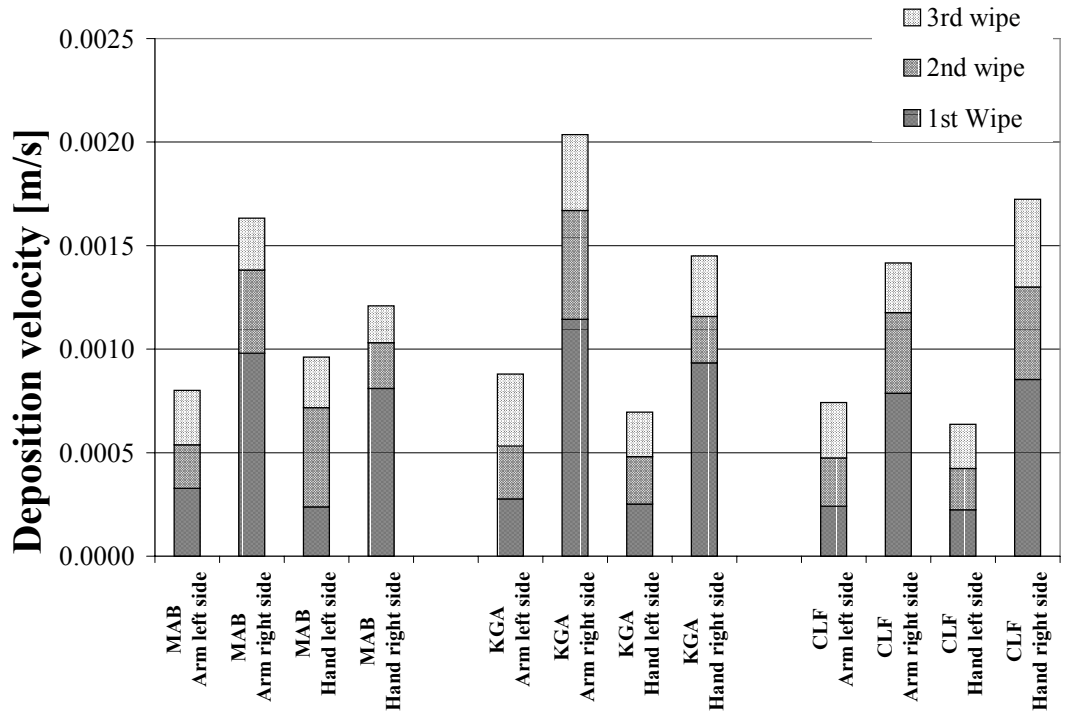

Figure 4.2 Deposition velocities for 2.5 µm dysprosium particles obtained by three sequential skin wipes on four locations on three different test persons in office test 11. The left side was wiped after the test persons had washed their hands.

Table 4.5 Removal efficiency by hand washing.

Experiment	Indium labelled 0.5 µm	Dysprosium labelled 2.5 µm	Europium labelled 10 µm
Office 10	0.19±0.05	0.38±0.14	0.29±0.25
Office 11	0.06±0.36	0.48±0.15	0.33±0.26

In addition to the 2.5 micron particles used in the previous Office experiments, 3 and 4.5 µm dysprosium labelled particles were also used to determine deposition velocities. Together with the indium and europium labelled particles this yielded results for 0.5, 2.5, 3, 4.5 and 10 µm particles. In Figure 4.3 the deposition velocities are plotted as a function of the particle size. As in previous experiments, a linear relationship is observed.

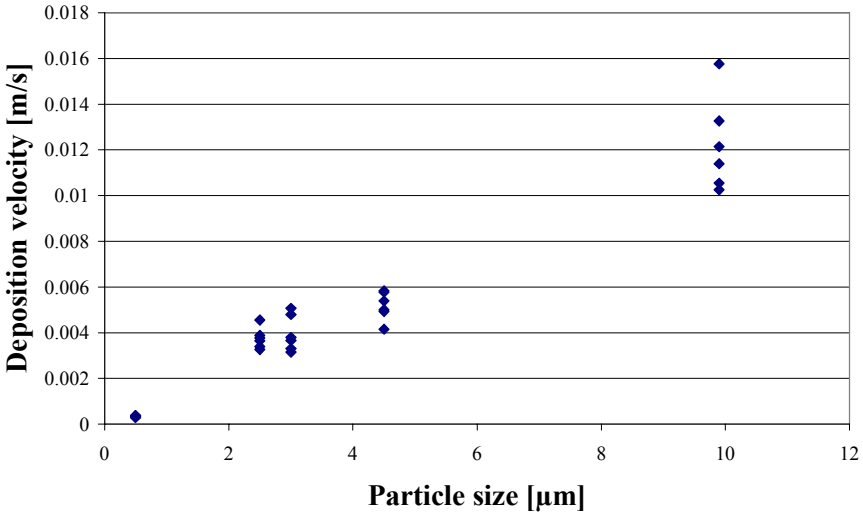

Figure 4.3 Review of the deposition velocity results obtained for the Office 9 to 16 experiments. Each point shows the average deposition velocity to all test persons in one test.

The average deposition velocities obtained for the three test persons are shown in Table 4.6, for two tracer particle sizes. There was no statistically significant difference between the deposition velocities found for the three test persons. Specifically, the significant difference between the test persons CLF and KGA that was observed in the earlier measurements was not observed here.

It should be noted that in test series 9-16, there were only two sampling locations on the volunteers, i.e. hands and arms, and both on the upward-facing side. No difference was observed between the two locations and the average values are presented in Table 4.6. This similarity was not surprising as the two locations were close together and had identical orientations.

Table 4.6 Average deposition velocity for the Office 9 to 16 experiments.

Test person	Number of sample locations	0.5 µm Indium [10^{-4} m s^{-1}]	2.5 µm Dysprosium [10^{-4} m s^{-1}]
MAB	16	3.0±1.2	36.4±21.8
CLF	16	3.6±1.1	35.1±14.6
KGA	16	3.2±1.0	35.1±15.3
Office 9–16 avg.	**48**	**3.3±1.1**	**35.5±17.7**

Exposure-tracer recovery relationship

In order to examine the relation between the integrated air concentration and the amount of recovered tracer, the exposure times and the amount of emitted aerosols were varied from test to test. It should be noted that the deposition velocity, by definition, is independent of the actual levels of exposure. The amount of recovered tracer (measured as tracer mass per unit skin area) was plotted as a function of the integrated air concentration (measured as tracer mass multiplied by the sampling time and divided by the sampled air volume) in Figure 4.4 for the 0.5 µm particles and in Figure 4.5 for the 2.5 µm particles. In this way an examination can be made of whether a linear relation between the integrated air concentration and the deposited tracer mass exists and thus

whether it is a good model to use a uniform deposition velocity for a given particle size.

For the 0.5 µm particles Figure 4.4 shows a linear relation (r=0.98) with the intercept being close to zero when the data presented in the midterm report is reviewed (represented by the diamonds in Figure 4.4). The slope of the regression line represents the deposition velocity. This slope is 0.00016±0.00002 m s^{-1}. The result of the first new Office experiment, Office 9, lies on the same line as the previous data (r = 0.98). However, the results from the later tests show higher surface contamination levels and the correlation coefficient is reduced (r = 0.85). This result indicates that the test room may have contained a residual tracer aerosol concentration from previous experiments, a possibility supported by the fact that the indium particles were very difficult to remove by hand washing. A background from previous experiments would lead to an overestimation of the deposition velocity, but it would also imply that the wiping efficiency had been overestimated, thus resulting in an underestimation the deposition velocity. Overall, an estimate of a deposition velocity range of 0.00015 to 0.0003 m s^{-1} is considered reasonable for particles in the size range 0.5 to 1 µm.

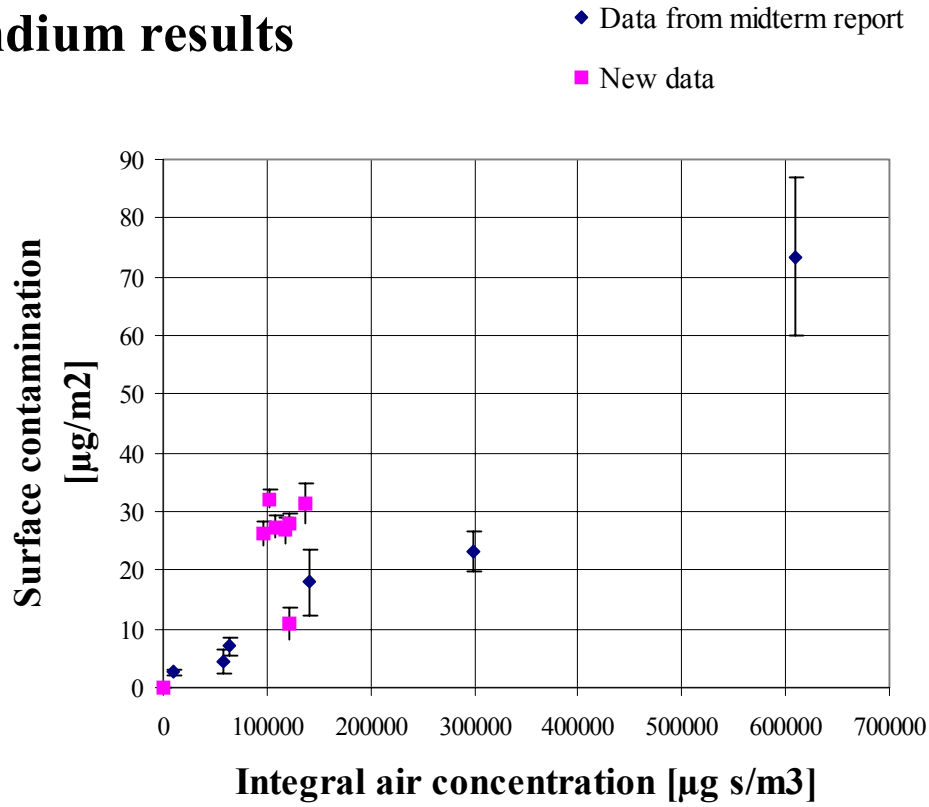

Figure 4.4 Surface contamination plotted versus the integrated air concentration in 8 different tests. The error bars show the standard deviation on the mean for each test.

For the 2.5 µm particles a less ideal result is seen in Figure 4.5. Here, a regression on the early data (shown as diamonds in the Figure 4.5) has a lower correlation factor (r=0.84) and the intercept is different from zero suggesting that there is a background of tracer particles on the skin wipes. However, an intercept of zero still lies within the 95% confidence interval. Addition of the new data did not improve the result.

Since sampling from unexposed persons has not shown any tracer background, it is likely that the results shown in Figure 4.5 are indicative of the natural variability of the deposition velocity. It should be noted that for the 0.5 μm particles, a variation in integrated air concentration over almost two orders of magnitude was recorded, whereas only a variation by a factor of 3 was registered for the 2.5 micron particles. During the new series of office experiments extra amounts of dysprosium were released in order to achieve a higher exposure level. However, the achieved integral air concentration was only 25 % above the former maximum and the variation in the integral air concentration is still smaller than desirable.

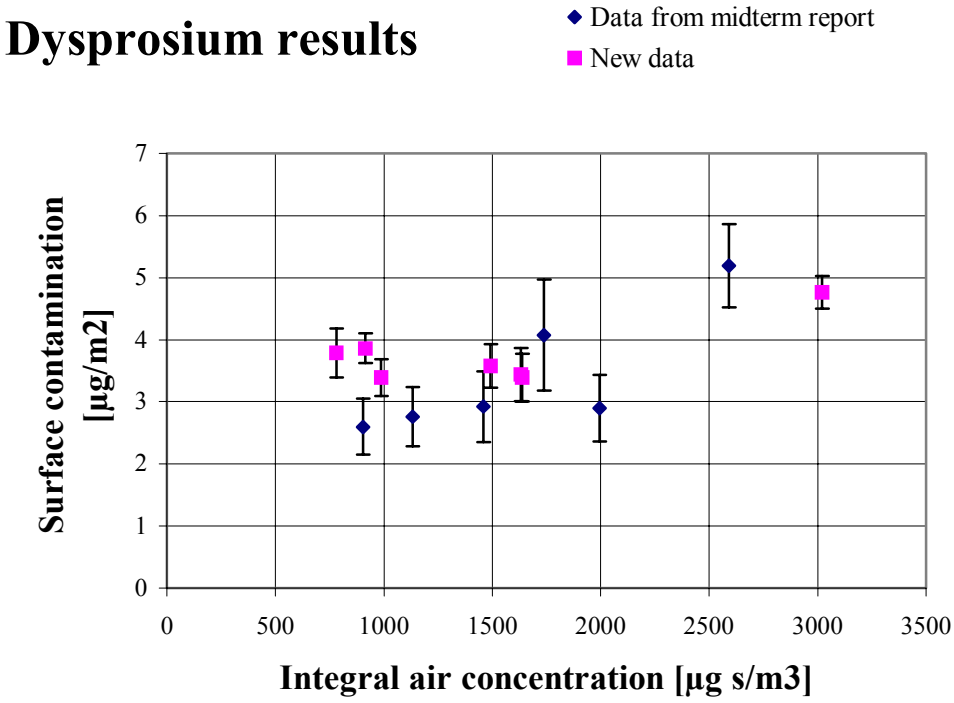

Figure 4.5 Surface contamination plotted versus the integral air concentration in 7 different tests with 2.5 μm particles. The error bars show the standard deviation on the mean for each test.

Another result that supports the assumption that there is a higher variability in the deposition of the larger particles is the deposition pattern on filter papers attached to surfaces in the room: walls, ceiling and floor. Although these filter papers show no tracer background, there is still a large variability in deposited tracer amounts from test to test. An example of the deposition on filter papers in two different positions is shown in Figure 4.6. It can be seen that in some cases the y-intercept is close to zero (the ceiling position) whereas there is an intercept significantly different from zero in other cases.

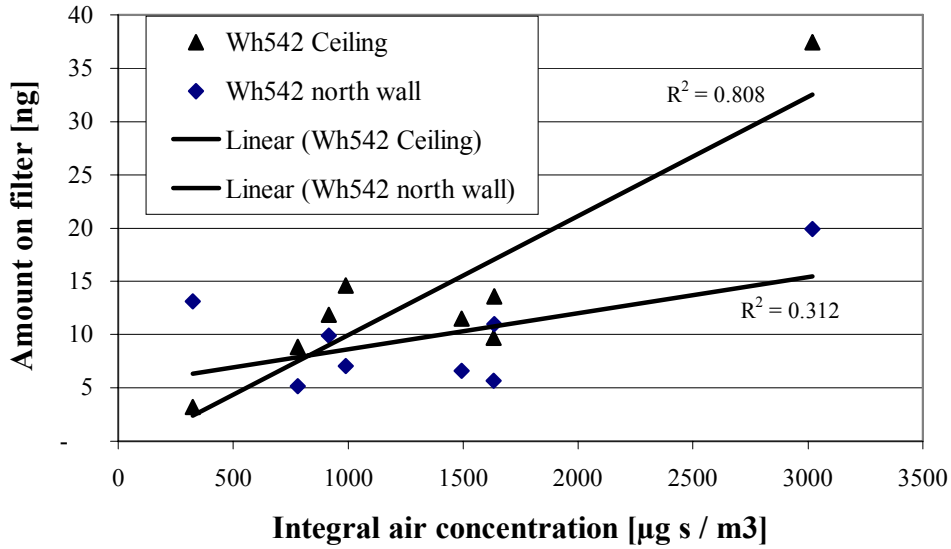

Figure 4.6 Variability of deposition of Dy-labelled particles passively sampled on Whatman filter papers (5cm ø) in the Office 9 to 16 tests.

In summary, the results obtained in realistic indoor environments were in good agreement with the test chamber results. In general the deposition velocity increased with increasing particle size. For the 2.5 µm particles the deposition velocity was 25 to 50 % higher in the test chamber than in the realistic environments, but this can be attributed to the variability due to different tests persons being exposed and the different air flow patterns in the two environments.

4.3 Factors relevant to the outdoor environment

Although the human population spends the majority of its time indoors, it is obviously also important, in the event of a nuclear accident, to assess the risk, from dermally deposited particulates, to those engaged in outdoor activities. Wind tunnels are commonly used to carry out controlled experiments under simulated outdoor conditions, and other workers (e.g. Gudmundson *et al.,* 1992) have carried out aerosol deposition measurements on human phantoms under elevated air velocity conditions. However, no experiments have yet been carried out using anthropomorphic bodies which are heated to human body temperature. In the present work, it was intended that measurements of tracer aerosol deposition velocities would be made to the surface of the heated cylinder which had been used in the test chamber experiments described earlier. However, the wind tunnel available was of the non-recirculating type and it was anticipated that it would require an experimental duration of several hours before an appreciable quantity of tracer aerosol sweeping past a body would be deposited at a detectable level. The use of the labelled silica particles employed in the indoor experiments was considered prohibitively expensive for the wind tunnel tests and a more economical alternative is described below.

An aerosol generator developed for the study of aerosol deposition onto forest canopies, as described by Kinnersley (1997), was used for the wind tunnel deposition experiments. Uranium aerosol is generated as follows: nine sidestream nebulisers connected to a clean air supply deliver nebulised uranyl acetate (depleted) from an aqueous solution to a conical expansion chamber, where the nebulised aerosol particles are mixed with diluting air. The aerosol then passes a radioactive charge neutralising source (74 MBq ^{85}Kr) and enters a fur-

nace, where residual water is removed from the particles. A delivery tube connects the generator to the wind tunnel.

Using the system described above, uranyl acetate aerosol particles with an aerodynamic diameter of 1.0 μm and a geometric standard deviation (σ_g) of 1.26 were generated. Wind tunnel experiments were then carried out, at windspeeds of 2 m s^{-1} and 4 m s^{-1}, to determine the deposition velocity of those particles to felt surfaces attached to the surface of the aluminium cylinder which was used in the test chamber experiments. The cylinder was heated to body temperature.

The technique chosen to analyse the felt surfaces for deposited aerosol was Delayed Neutron Counting (DNC). DNC makes use of the fact that a fissile element (such as ^{235}U or ^{239}P) may undergo fission when bombarded by a neutron flux, producing unstable isotopes which may decay by the emission of a beta-particle to form an unstable species which is neutron rich. This unstable nucleus may then decay by the emission of a neutron (Benzing *et. al,* 1993); the half-life of the second emission is extremely short ($T_{1/2} \sim 10^{-20}$s) which makes it seem that the half-life of the neutron decay is the same as the beta decay. The beta decay processes have half-lives ranging from a fraction of a second to approximately 1 minute.

The samples were irradiated in a neutron flux of 1 x 10^{12} n cm^{-2} s^{-1} and delivered by an automated system to an array of nine BF_3 detectors. The quantity of uranyl acetate present in the samples was deduced by comparing the neutron spectrum with that of the reference standard which contains 100 mg of uranium nitrate.

The results of the wind tunnel experiments are presented in Table 4.7. A significant increase in deposition velocity with increasing wind speed is indicated, as should be expected for particles that are susceptible to inertia effects. This can be compared to the measured deposition velocity on the cylinder under the low air velocity conditions in the test chamber (0.25 m s^{-1}), where a deposition velocity of 3.3 x 10^{-4} m s^{-1} was found for 2.5 μm particles.

Table 4.7 Aerosol deposition velocities measured on the cylinder surfaces in the wind tunnel.

	Wind speed [m s^{-1}]	
	2	4
Deposition velocity [10^{-4} m s^{-1}]	55-81	84-136
No. of samples	16	11

Conclusion

In work package 3, deposition velocities have been measured for three particle sizes in a test chamber and two particle sizes in realistic indoor environments. The effect of electrical grounding and heat-generated turbulence on deposition has been examined. Deposition velocities on a heated cylinder and from human body surfaces have been compared. Overall, a coherent data set of skin deposition velocities has been compiled.

A wind tunnel has been used to simulate outdoor conditions. The experiment performed showed a clear increase in deposition velocity with increasing wind speed.

In Figure 4.7 the different deposition velocities obtained in various test environments have been presented together. The 'normal' condition test chamber experiments and the realistic indoor environments indicate that there is a linear increase in deposition velocity with particle size. The grounding of the arm was

seen to reduce deposition somewhat. For outdoor conditions there is a significant increase in deposition by almost an order of magnitude compared to the expected value for 1 μm particles. The results from the last year of the project can be seen to fit into the overall pattern.

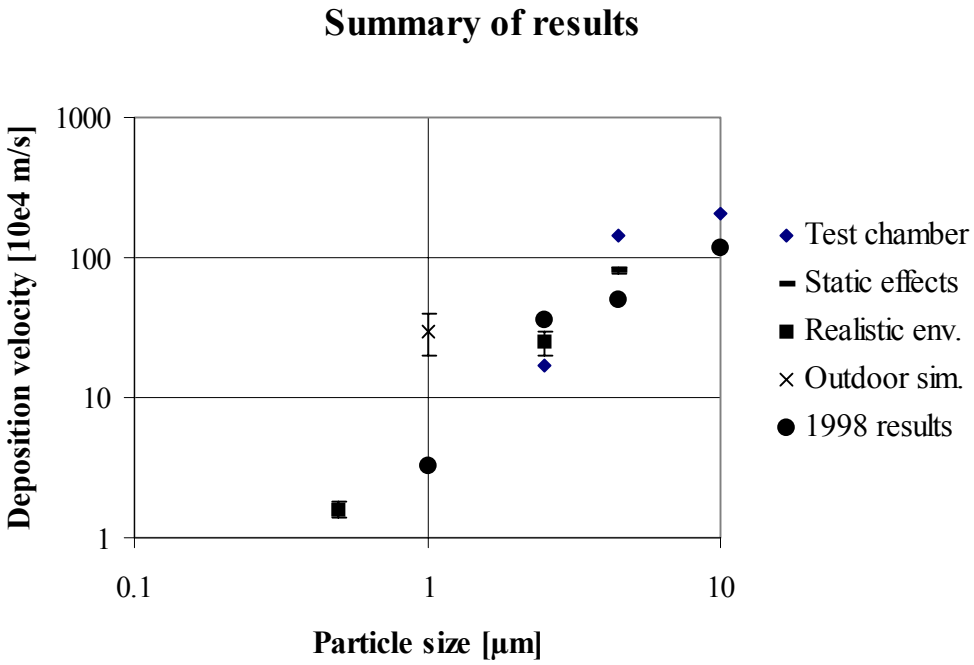

Figure 4.7 Review of deposition results to skin under different conditions.

5 Doses received from contamination of skin and clothing

The parameters obtained from the experimental work in this study have been used to model the dose from deposits on skin, clothing and hair after an accidental release of radionuclides. To facilitate a comparison of the doses received from direct deposition to humans with doses received through other pathways (e.g., external radiation from the environment), the modelled doses are reported in figures relative to the dry deposition of 1 MBq m^{-2} of the investigated isotopes to a reference surface (a cut grassed lawn). Both the skin dose from β- and γ-emitters and the whole body dose from γ-emitters have been considered.

The model was also applied together with near-surface air concentrations of various contaminants measured after the Chernobyl accident (Kryshev, 1996) to calculate the doses received by dry deposition to humans in Novozybkov, Russia over the first two months following the Chernobyl release. The time-integrated air-concentrations of the measurable particles in Novozybkov are shown in Table 5.1.

The above reference does not distinguish between the different chemical forms of iodine. However, the COSYMA model suggests that 99% of the iodine is in the elemental form (with a dry deposition velocity of 0.01 m s^{-1}), while the remaining 1% is in organic form (deposition velocity: $5 \cdot 10^{-4}$ m s^{-1}) and this partitioning has been assumed in the present work.

It should be considered that the concentration of aerosol in the Novozybkov area was greatly depleted by rain, which led to high ground contamination levels. However, it followed from the air concentrations and from measured deposition velocities to a lawn (Roed, 1990) that the contribution to the ground contamination level from *dry* deposition of ^{137}Cs in the area (the nuclide which essentially determines the long-term doses from the ground) was only about 8 kBq/m^2.

With the exception of iodine, for which the chemistry is more complex, the different contaminant aerosol was divided into two groups : the volatile group (^{132}Te, ^{134}Cs, ^{137}Cs, ^{99}Mo, ^{103} Ru and ^{106}Ru) with lower Activity Median Aerodynamic Diameter (AMAD) values of the order of 0.7 μm and the refractory group with higher AMAD values of the order of 4 μm, to which ^{140}Ba, ^{95}Zr, ^{141}Ce, ^{144}Ce, ^{89}Sr and ^{90}Sr belong (Reineking *et al.*, 1987; Rulik *et al.*, 1989; Dorrian, 1997).

As indicated above, the dry deposition velocities of the different contaminant aerosol to a grassed lawn were estimated from field measurements made shortly after the Chernobyl accident (Roed, 1990) and from COSYMA parameters. The estimates of dry deposition velocities to skin were based on the results obtained in the current project.

It was assumed in the calculations that the people in the area stayed indoors during virtually the entire deposition phase. The relationship between the indoor and outdoor air concentrations (C_i / C_o) was found from the following expression:

$$C_i / C_o = f \cdot \lambda_r / (\lambda_r + \lambda_d)$$

(Roed & Cannell, 1987), where λ_r is the fraction of air exchanged per unit of time, λ_d is the fraction of aerosols indoors depositing per unit of time and f is the filtering factor (the fraction of aerosols in air entering the building which is not retained in cracks and fissures of the building structure).

Numerous experiments (Fogh *et al.*, 1997) have shown that the filtering factor can be assumed to be 1 and that a realistic value of λ_r is 0.4 h^{-1} for western European houses of good construction. Further, it was estimated from the experimental data that λ_d would be in the order of 3 h^{-1} for aerosols of the refractory group and 0.4 h^{-1} for most of the volatiles, with the exception of the rutheniums, for which λ_d was estimated to be 1.1 h^{-1} and of iodine, for which the λ_d estimate was based on the publications of Kocher (1980) and Roed & Cannell (1987). The corresponding C_i / C_o relationships can be seen in Table 5.1. The total integrated skin deposition (kBq/m^2) was calculated by multiplication of the time-integrated air concentrations by the indoor/outdoor relationship and the skin deposition velocities. These values are also listed in Table 5.1.

A 'half-life correction' was then introduced, taking into account both the radioactive decay half-lives of the isotopes and a 'clearance' half life, by which the skin contaminant concentration is depleted over the first year. This 'half-life correction' is a critical parameter in the dose calculations. Recent findings within the project suggest that the 'clearance' half-life is about 1.2 days for 2.5 μm particles and only about 0.16 days for 4.5 μm particles. In other words: the 'clearance' half-life increases by a factor of about 7.5 as the particle size decreases from 4.5 μm to 2.5 μm. Based on these experimental results and reported indoor resuspension rates for different particle sizes (Thatcher & Layton, 1995), it would be expected that the 'clearance' half-life of 1 μm particles would be one or two orders of magnitude greater than that found for the 2.5 μm particles, i.e. 10-100 days. The clearance is, however, here likely to be governed by the shedding of the stratum corneum over a few weeks, although especially small particles may migrate to deeper skin crevices and hair follicles.

The COSYMA modellers assume the 'clearance' half-life to generally be of the order of 30 days, and this value was applied in the calculations for the small (sub-micron) particles.

It was assumed that a fraction of the body would be covered by clothing. For the clothing, the clearance half-life was based on results obtained within the project. It was found that ordinary washing of cotton would lead to a reduction of the contamination level by a factor of at least ca. 1.4. The washing effect did not appear to be greatly influenced by the particle size in the 0.5-2.5 µm range, although a tendency was observed towards a greater effect for the larger particles. If it is assumed that the clothes are washed at 2 days intervals, a washing reduction factor of 1.4 corresponds to a clearance half-life of 3.9 days, which was applied in the calculations. The deposition velocities to clothing were evaluated from results of the current project and from results reported by Lange (1995).

5.1 Gamma Doses

For estimation of the dose contribution to the body from gamma emission on skin, Monte Carlo calculations were performed using the MCNP code. A simplified model was applied, in which a tissue equivalent ICRP sphere was irradiated by a surface contamination of variable energy. It was found that the sensitivity of this model towards changes in sphere diameter was low. In the model the sphere was placed at a height of 1m above ground. Figure 5.1 shows the energy dependence of the gamma doses received per gamma ray emitted each second from an area of 1 cm^2. The relative uncertainty on the Monte Carlo calculations shown in Figure 5.1 was in all cases less than 1%.

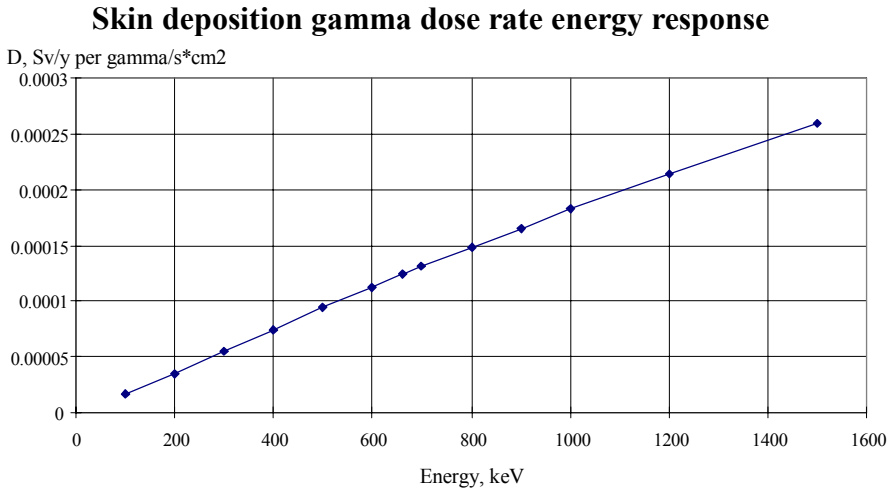

Figure 5.1 Monte Carlo modelled whole-body gamma doses received from skin contamination. Dose responses as a function of gamma ray energy.

In the calculations it was assumed that the fraction of the skin of a person that is directly exposed corresponds to the fraction of the total skin constituted by the hands and the head (0.15, according to the report of the Task Group on Reference Man (ICRP 23, 1974)). The rest of the body is assumed to be covered by clothes. The results for skin are shown in Table 5.1.

Table 5.2 shows the corresponding results of the calculations of gamma doses from contamination on clothing.

Table 5.1 Parameters applied in the calculations of doses received from gamma emission from skin contamination. For each isotope that was measured in near-ground level air in Novozybkov by Kryshev (1996), the following factors are given: radioactive half-life, AMAD, indoor/outdoor air concentration, deposition velocity to skin and to grassed lawn, half-life correction factor and the dose rate conversion factor based on Monte Carlo calculations and the fraction of skin directly exposed (0.15). For reference, the resultant gamma dose contributions from skin deposition are given per unit of surface contamination on a cut, grassed lawn. The last three columns show the integrated air concentrations as measured by Kryshev, the corresponding skin deposition and resultant gamma doses.

Isotope	T½ [days]	AMAD [μm]	Ci/Co [ ]	V_d, face/hand [m s^{-1}]	V_d grass [m s^{-1}]	Half-life correct. [ ]	Dose rate [Sv y^{-1} per Bq cm^{-2} exposed]	Relative dose [mSv per MBq/m^2 of isotope on grass]	Integr. air contam. (Kryshev) [Bq s m^{-3}]	Contam. on skin (Kryshev) [Bq m^{-2}]	Dose based on deposit. figures of Kryshev [Sv]
I-131 (organic)	8	0.5	0.36	0.005	5.00E-04	0.0249	1.02E-05	2.08E-02	1.79E+06	3222	8.20E-08
Te-132	3.25	0.7	0.5	0.001	4.30E-04	0.0115	5.25E-06	7.08E-03	1.81E+07	9050	5.51E-08
Cs-134	767	0.7	0.5	0.001	4.30E-04	0.1140	3.41E-05	4.52E-01	8.93E+06	4465	1.73E-06
Cs-137	10986.5	0.7	0.5	0.001	4.30E-04	0.1182	1.53E-05	2.10E-01	1.78E+07	8900	1.61E-06
Ba-140	12.8	4	0.12	0.012	7.50E-04	0.0006	3.53E-06	4.23E-04	1.08E+07	15552	3.42E-09
Zr-95	65.5	4	0.12	0.012	7.50E-04	0.0006	2.04E-05	2.47E-03	2.67E+06	3844.8	4.95E-09
Mo-99	2.75	0.7	0.5	0.001	4.30E-04	0.0099	3.99E-06	4.62E-03	5.18E+06	2590	1.03E-08
Ru-103	39.6	0.7	0.27	0.001	4.10E-04	0.0674	1.31E-05	5.80E-02	9.10E+06	2457	2.16E-07
Ru-106	369	0.7	0.27	0.001	4.10E-04	0.1096	4.80E-06	3.47E-02	2.28E+06	615.6	3.24E-08
Ce-141	32.5	4	0.12	0.012	7.50E-04	0.0006	1.65E-06	1.99E-04	3.17E+06	4564.8	4.74E-10
Ce-144	284.4	4	0.12	0.012	7.50E-04	0.0006	4.80E-07	5.83E-05	2.14E+06	3081.6	9.35E-11
Sr-89	50.5	4	0.12	0.012	7.50E-04	0.0006	0	0	1.32E+05	190.08	0
Sr-90	10585	4	0.12	0.012	7.50E-04	0.0006	0	0	1.41E+04	20.304	0
Np-239	2.4	4	0.12	0.012	7.50E-04	0.0005	1.80E-06	2.05E-04	1.68E+07	24192	2.58E-09
I-131 (elem.)	8		0.07	0.010	1.00E-02	0.0249	1.02E-05	1.78E-03	1.77E+08	123900	3.15E-06

Table 5.2 Parameters applied in the calculations of doses received from gamma emission from contamination on clothing. For each isotope that was measured in near-ground level air in Novozybkov by Kryshev (1996), the following factors are given: radioactive half-life, AMAD, indoor/outdoor air concentration, deposition velocity to clothing and to grassed lawn, half-life correction factor and the dose rate conversion factor based on Monte Carlo calculations and the fraction of the body covered by clothing (0.80). For reference, the resultant gamma dose contributions from deposition to clothing are given per unit of surface contamination on a cut, grassed lawn. The last three columns show the integrated air concentrations as measured by Kryshev, the corresponding deposition to clothing and resultant gamma doses.

Isotope	T½ [days]	AMAD [μm]	Ci/Co [ ]	V_d clothing [m s^{-1}]	V_d grass [m s^{-1}]	Half-life correct. [ ]	Dose rate [Sv y^{-1} per Bq cm^{-2} exposed]	Relative dose [mSv per MBq/m^2 of isotope on grass]	Integr. air contam. (Kryshev) [Bq s m^{-3}]	Contam. on clothing (Kryshev) [Bq m^{-2}]	Dose based on deposit. figures of Kryshev [Sv]
I-131 or	8	0.5	0.36	1.00E-03	5.00E-04	0.0103	5.78E-05	4.90E-02	1.79E+06	6.44E+02	3.86E-08
Te-132	3.25	0.7	0.5	1.70E-03	4.30E-04	0.0070	2.98E-05	2.42E-02	1.81E+07	1.54E+04	3.21E-07
Cs-134	767	0.7	0.5	1.70E-03	4.30E-04	0.0153	1.93E-04	3.44E-01	8.93E+06	7.59E+03	2.25E-06
Cs-137	10986.	0.7	0.5	1.70E-03	4.30E-04	0.0154	8.67E-05	1.55E-01	1.78E+07	1.51E+04	2.02E-06
Ba-140	12.8	4	0.12	2.70E-03	7.50E-04	0.0118	2.00E-05	4.53E-02	1.08E+07	3.50E+03	8.26E-08
Zr-95	65.5	4	0.12	2.70E-03	7.50E-04	0.0145	1.16E-04	3.23E-01	2.67E+06	8.65E+02	1.45E-07
Mo-99	2.75	0.7	0.5	1.70E-03	4.30E-04	0.0063	2.26E-05	1.68E-02	5.18E+06	4.40E+03	6.34E-08
Ru-103	39.6	0.7	0.27	1.70E-03	4.10E-04	0.0140	7.40E-05	6.83E-02	9.10E+06	4.18E+03	4.34E-07
Ru-106	369	0.7	0.27	1.70E-03	4.10E-04	0.0152	2.72E-05	2.73E-02	2.28E+06	1.05E+03	4.36E-08
Ce-141	32.5	4	0.12	2.70E-03	7.50E-04	0.0137	9.35E-06	2.47E-02	3.17E+06	1.03E+03	1.33E-08
Ce-144	284.4	4	0.12	2.70E-03	7.50E-04	0.0152	2.72E-06	7.94E-03	2.14E+06	6.93E+02	2.87E-09
Sr-89	50.5	4	0.12	2.70E-03	7.50E-04	0.0143	0	0	1.32E+05	4.28E+01	0
Sr-90	10585	4	0.12	2.70E-03	7.50E-04	0.0154	0	0	1.41E+04	4.57E+00	0
Np-239	2.4	4	0.12	2.70E-03	7.50E-04	0.0058	1.02E-05	1.15E-02	1.68E+07	5.44E+03	3.26E-08
I-131 el.	8		0.07	1.00E-02	1.00E-02	0.0103	5.78E-05	4.19E-03	1.77E+08	1.24E+05	7.43E-06

5.2 Beta Doses

Another dose contribution from contamination deposited on skin results from beta radiation. The calculations of this contribution required knowledge of the dose rate to the basal layer of the epidermis for the different isotopes. Nuclide-specific absorbed dose rates at an epidermis equivalent depth in water (ca. 70 μm) from various beta sources were derived from the figures stated in ICRU report 56 (1997). The ICRU figures were mostly based on the Monte Carlo calculations of Cross et al. (1992). The results are shown in Table 5.3. These dose rate factors were found to be in fairly good agreement with the corresponding factors reported by Faw (1992).

By multiplication of the skin contamination levels by the 'half-life correction factor' and the dose rate factors for beta exposure at a depth of 70 μm, the total doses to the skin were found. Also presented in Table 5.3 are the doses weighted by a factor of $0.01 \cdot 0.15$, corresponding to respectively the tissue weighting factor for skin (according to ICRP 60, 1990) and the fraction of the total skin constituted by the hands and the head. Results are presented relative to a 1 MBq m^{-2} dry deposition of each of the examined isotopes to a cut grassed lawn, and also in relation to the specific Novozybkov example described above.

Table 5.3 Parameters applied in the calculations of doses received from beta emission from skin contamination. For each isotope that was measured in near-ground level air in Novozybkov by Kryshev (1996), the following factors are given: radioactive half-life, AMAD, indoor/outdoor air concentration, deposition velocity to skin, half-life correction factor and the dose rate conversion factor based on ICRU-56. For reference, the resultant beta dose contributions from skin deposition are given per unit of surface contamination on a cut, grassed lawn. The last four columns show the integrated air concentrations as measured by Kryshev, the corresponding skin deposition and resultant unweighted and weighted beta doses.

Isotope	T½ [days]	AMAD [μm]	Ci/Co [ ]	V_d, face/ hand [m s^{-1}]	Dose rate at 70 μm -ICRU56 [Sv y^{-1} per Bq cm^{-2}]	Half-life correct. [ ]	Relative dose [Sv per MBq/m^2 of isotope on grass]	Integr. air contam. (Kryshev) [Bq s m^{-3}]	Contam on skin (Kryshev) [Bq m^{-2}]	Total skin dose (Kryshev) [Sv]	Dose total tissue/% weighted (Kryshev) [Sv]
I-131 or	8	0.5	0.36	5.00E-03	0.012	0.0249	2.45E-02	1.79E+06	3222	9.65E-05	1.45E-07
Te-132	3.25	0.7	0.5	1.00E-03	0.0079	0.0115	1.06E-02	1.81E+07	9050	8.29E-05	1.24E-07
Cs-134	767	0.7	0.5	1.00E-03	0.0094	0.1140	1.25E-01	8.93E+06	4465	0.000479	7.18E-07
Cs-137	10986.5	0.7	0.5	1.00E-03	0.014	0.1182	1.92E-01	1.78E+07	8900	0.001473	2.21E-06
Ba-140	12.8	4	0.12	1.20E-02	0.013	0.0006	1.56E-03	1.08E+07	15552	1.26E-05	1.9E-08
Zr-95	65.5	4	0.12	1.20E-02	0.01	0.0006	1.21E-03	2.67E+06	3844.8	2.43E-06	3.64E-09
Mo-99	2.75	0.7	0.5	1.00E-03	0.013	0.0099	1.51E-02	5.18E+06	2590	3.35E-05	5.03E-08
Ru-103	39.6	0.7	0.27	1.00E-03	0.0054	0.0674	2.40E-02	9.10E+06	2457	8.95E-05	1.34E-07
Ru-106	369	0.7	0.27	1.00E-03	0.016	0.1096	1.16E-01	2.28E+06	615.6	0.000108	1.62E-07
Ce-141	32.5	4	0.12	1.20E-02	0.014	0.0006	1.69E-03	3.17E+06	4564.8	4.02E-06	6.03E-09
Ce-144	284.4	4	0.12	1.20E-02	0.0079	0.0006	9.59E-04	2.14E+06	3081.6	1.54E-06	2.31E-09
Sr-89	50.5	4	0.12	1.20E-02	0.015	0.0006	1.81E-03	1.32E+05	190.08	1.8E-07	2.69E-10
Sr-90	10585	4	0.12	1.20E-02	0.013	0.0006	1.58E-03	1.41E+04	20.304	1.67E-08	2.5E-11
Np-239	2.4	4	0.12	1.20E-02	0.015	0.0005	1.71E-03	1.68E+07	24192	2.15E-05	3.23E-08
I-131 el.	8		0.07	1.00E-02	0.012	0.0249	2.10E-03	1.77E+08	123900	0.003712	5.57E-06

On the parts of the body that are covered by clothes, the beta skin doses are much lower due to the shielding effect of the clothing. The Tables in Appendix A of ICRU report 56 show that due to the similar beta attenuation characteristics, it is reasonable to assume that equal mass-thicknesses of clothing and tissue are equivalent in dose considerations. From the dose rate factors given in ICRU 56 it followed that practically no beta doses would be received through 3 mm thick clothing. The numbers presented in Table 5.4 express the doses that would be received through 0.4 mm thick clothing.

The dose rate factors found for 0.4 mm clothing were in reasonable agreement with those reported by Taylor et al. (1997) for a 26 mg cm^{-2} thick layer of cotton with a density of 0.7 g cm^{-3}. Taylor et al. also demonstrated that an air gap of 1 cm between the skin and the clothing could halve the doses received from beta radiation with higher energies (above 0.4 MeV).

As before, both the total doses to the skin epidermis and the weighted dose (by tissue weight factor and percentage of skin covered) are shown in Table 5.4.

Table 5.4. Parameters applied in the calculations of doses received from beta emission from contamination on clothing. For each isotope that was measured in near-ground level air in Novozybkov by Kryshev (1996), the following factors are given: radioactive half-life, AMAD, indoor/outdoor air concentration, deposition velocity to clothing, half-life correction factor and a dose rate conversion factor based on ICRU-56. For reference, the resultant beta dose contributions from deposition on clothing are given per unit of surface contamination on a cut, grassed lawn. The last four columns show the integrated air concentrations as measured by Kryshev, the corresponding deposition on clothing and resultant un-weighted and weighted beta doses.

Isotope	T½ [days]	AMAD [μm]	Ci/Co [ ]	V_d clothing [m s^{-1}]	Dose rate at 0.4 mm (ICRU56) [Sv y^{-1} per Bq cm^{-2}]	Half-life correct. [ ]	Relative dose [Sv per MBq/m^2 of isotope on grass]	Integr. air contam. (Kryshev) [Bq s m^{-3}]	Contam. on clothing (Kryshev) [Bq m^{-2}]	Total skin dose (Kryshev) [Sv]	Dose total tissue/% weighted (Kryshev) [Sv]
I-131 or	8	0.5	0.36	1.00E-03	0.00263	0.0103	4.47E-04	1.79E+06	6.44E+02	1.76E-06	1.41E-08
Te-132	3.25	0.7	0.5	1.70E-03	5.78E-5	0.0070	8.01E-05	1.81E+07	1.54E+04	6.23E-07	4.99E-09
Cs-134	767	0.7	0.5	1.70E-03	0.00227	0.0153	6.91E-03	8.93E+06	7.59E+03	2.65E-05	2.12E-07
Cs-137	10986.5	0.7	0.5	1.70E-03	0.00337	0.0154	1.03E-02	1.78E+07	1.51E+04	7.86E-05	6.29E-07
Ba-140	12.8	4	0.12	2.70E-03	0.00428	0.0118	2.19E-03	1.08E+07	3.50E+03	1.77E-05	1.42E-07
Zr-95	65.5	4	0.12	2.70E-03	0.00075	0.0145	4.73E-04	2.67E+06	8.65E+02	9.47E-07	7.58E-09
Mo-99	2.75	0.7	0.5	1.70E-03	0.00589	0.0063	7.43E-03	5.18E+06	4.40E+03	1.65E-05	1.32E-07
Ru-103	39.6	0.7	0.27	1.70E-03	0.00024	0.0140	3.81E-04	9.10E+06	4.18E+03	1.42E-06	1.14E-08
Ru-106	369	0.7	0.27	1.70E-03	0.01082	0.0152	1.85E-02	2.28E+06	1.05E+03	1.73E-05	1.38E-07
Ce-141	32.5	4	0.12	2.70E-03	0.00148	0.0137	8.80E-04	3.17E+06	1.03E+03	2.09E-06	1.67E-08
Ce-144	284.4	4	0.12	2.70E-03	0.00025	0.0152	1.65E-04	2.14E+06	6.93E+02	2.64E-07	2.11E-09
Sr-89	50.5	4	0.12	2.70E-03	0.00784	0.0143	4.85E-03	1.32E+05	4.28E+01	4.8E-07	3.84E-09
Sr-90	10585	4	0.12	2.70E-03	0.00291	0.0154	1.94E-03	1.41E+04	4.57E+00	2.05E-08	1.64E-10
Np-239	2.4	4	0.12	2.70E-03	~0	0.0058	0.00E+00	1.68E+07	5.44E+03	0	0
I-131el.	8		0.07	1.00E-02	0.00263	0.0103	1.91E-04	1.77E+08	1.24E+05	0.000339	2.71E-06

For simplicity, hair has not been considered in the modelling. Results obtained within the project suggest that deposition velocities of sub-micron particles to hair may be higher than those to skin. However, the deposition velocity to a swimming cap was found to be similar to that to hair. In any case, measurements of hair contamination clearance suggest that ordinary hair wash can remove most of the contamination, even with small particles, as represented by indium. Since the most of the contamination on hair would be deposited at freely exposed distal hair ends (Lange, 1995), it would be expected that the extra distance and attenuation in hair would significantly reduce dose contributions from beta radiation.

This means that excluding the hair would probably make both gamma and beta dose estimates conservative. together with the extra distance and shielding provided by the hair, would make The calculations of Rohloff and Heinzelmann (1996) clearly demonstrate that the dose rates received by photon radiation to the basal layer of the skin epidermis are negligible compared with the contributions from beta radiation.

Skin contact transfer

Another type of skin exposure than that by airborne contamination may occur if skin comes into contact with contaminated surfaces (e.g., a table, to which aerosol deposition has occurred). The radiological significance of the contact transfer pathway of contaminants to skin depends on the time of contact transfer following deposition and in relation to this: the isotopic composition (e.g.,

short- or long-lived radionuclides). Another important factor is of course the fraction of the surface contamination that is transferred. This latter factor has been investigated experimentally in the project. Based on these experiments it is assumed in the calculations that about one quarter of the contamination may be transferred. The contamination layer on the surface from which the transfer was to occur was rather thin, as it originated from airborne deposition at approximately the same loading as was applied in the skin deposition studies. If the contaminant loading had been much greater (visible), the fraction transferred might well have been smaller. The moisture of the skin did not appear to greatly influence the fraction removed. If the contamination is 'smeared' off from a rather large surface, the transfer may be considerably greater than that measured, where the transfer was by simple contact. However, if the contamination were the result of a 'smearing', the skin contaminant dust layer would be considerably thicker and would probably have a much shorter skin clearance half-life component. Table 5.5 shows the contamination by contact transfer from a surface in Novozybkov (based on Kryshev's figures, as referenced above) after 3 days' deposition. Later on, long-lived radionuclide concentrations will build up, whereas the short-lived, such as ^{131}I will become less significant in relation to contact transfer. Average indoor dry deposition velocities were applied in the calculations. However, on some horizontal surfaces, the deposition velocity may be several times greater. The contact transfer is compared with the total airborne skin contamination over the period, and this relationship is also presented. As these figures indicate, contact transfer in this case does not have a very great bearing on the total dose received, but in other cases, where the contamination is not airborne, e.g. in connection with decommissioning of nuclear establishments, dust contact transfer may be a very important consideration.

Table 5.5. Skin contact transfer from an average indoor surface after 3 days of contaminant deposition in Novozybkov (Kryshev, 1996) following the Chernobyl accident. The contact transfer is compared with the total amount of contamination deposited to skin also in Novozybkov. The relationship between the contact transfer and deposited skin contamination under these circumstances is given. In the last two columns the contact transfer and deposited skin contamination are both given relative to the contamination level on the reference surface, a cut, grassed lawn.

Isotope	Total Integr. air contam. (Kryshev) [Bq s m^{-3}]	Indoor depos. (Kryshev) [Bq m^{-2}] after 3 d. with no removal	Contact transfer (3 days) (Kryshev) [Bq m^{-2}]	Contamination on skin (Kryshev) [Bq m^{-2}]	Relationship (Contact transfer/ deposit. contam.)	Contact transfer [Bqm^{-2} on skin per Bq m^{-2} on grass]	Deposited contam. [Bq m^{-2} on skin per Bq m^{-2} on grass]
I-131 or.	1.79E+06	5.16E+02	129	3222	0.040	3.27E-02	8.18E-01
Te-132	1.81E+07	4.34E+02	109	9050	0.012	1.40E-02	1.16E+00
Cs-134	8.93E+06	2.14E+02	53.6	4465	0.012	1.40E-02	1.16E+00
Cs-137	1.78E+07	4.27E+02	107	8900	0.012	1.40E-02	1.16E+00
Ba-140	1.08E+07	2.07E+02	51.8	15552	0.003	6.40E-03	1.92E+00
Zr-95	2.67E+06	5.13E+01	12.8	3844.8	0.003	6.40E-03	1.92E+00
Mo-99	5.18E+06	1.24E+02	31.1	2590	0.012	1.40E-02	1.16E+00
Ru-103	9.10E+06	1.18E+02	29.5	2457	0.012	7.90E-03	6.59E-01
Ru-106	2.28E+06	2.95E+01	7.39	615.6	0.012	7.90E-03	6.59E-01
Ce-141	3.17E+06	6.09E+01	15.2	4564.8	0.003	6.40E-03	1.92E+00
Ce-144	2.14E+06	4.11E+01	10.3	3081.6	0.003	6.40E-03	1.92E+00
Sr-89	1.32E+05	2.53E+00	0.634	190.08	0.003	6.40E-03	1.92E+00
Sr-90	1.41E+04	2.71E-01	0.067	20.304	0.003	6.40E-03	1.92E+00
Np-239	1.68E+07	3.23E+02	80.6	24192	0.003	6.40E-03	1.92E+00

I-131 el.	1.77E+08	9.91E+04	24812	123900	0.200	1.40E-02	7.00E-02

5.3 Conclusions on dose modelling

From Tables 5.1 and 5.2 it can be seen that with the given assumptions and air concentrations measured at Novozybkov, the total dose contribution received over a few months from gamma radiation from contamination on skin and clothing amounts to some 20 μSv. This can be compared with the external dose contribution from contamination on other surfaces in the environment (e.g., soil, roofs, walls of buildings and pavings), which, with a total deposition of only 8 kBq/m^2, as was assumed in these calculations, would be of the order of 10-50 μSv over the first year, depending on the degree of shielding provided by the dwellings (Andersson, 1996). The calculated skin doses are of the same order of magnitude as the committed doses from plume inhalation and greater than for instance the external doses received during the plume passage. Dry deposition after the Chernobyl accident actually led to contamination of living areas in Russia with levels which were several hundred times higher. Here the skin contamination would give a gamma dose of several mSv.

It follows from Table 5.3 that the dose from the beta radiation to the epidermal layer of the directly exposed skin is about 6 mSv, in total. With a contamination level several hundred times greater, the skin dose would be several Sv. According to ICRP publication 59 (1991) the threshold for acute radiation effects by exposure of large areas of skin is generally assumed to be about 20 Sv, although acute tissue breakdown has been reported for doses as low as 15 Sv. These doses should also be compared with the risk of skin cancer mortality, which is estimated to be 2 10^{-4} Sv^{-1}, and with the skin morbidity risk ($9.8 \cdot 10^{-2}$ Sv^{-1}), which is extremely high at doses of the range of a Sievert (ICRP 59, 1991).

The doses in the last column of Table 5.3 (total over isotopes=9.2 μSv), which were weighted with the skin tissue weight factor and the percentage of the body not covered by clothes, make it possible to evaluate the effect of the skin irradiation relative to that from irradiation of other organs. However, this weighting may result in an under-estimation of the skin cancer risks. ICRP 59 states that the stochastic risks are dependent on the exposure of the area to sunlight (UVR). An exposure of all the skin that is normally exposed to UVR is said to give a risk comparable to that for whole-body exposure.

The beta doses received through a layer of clothing of 0.4 mm in thickness were in the Novozybkov case study found to amount to a total of only about 0.5 mSv. In other words, a thin layer of regularly washed cotton can locally reduce the beta skin dose by a factor of about 10. As mentioned above this factor may be greater due to the air gap between the contaminated clothing and the skin.

Skin contact transfer does not appear to be of great significance compared with the other pathways of dose following an airborne deposition of contaminants. However, this pathway may be important in scenarios involving highly contaminated dust. The resultant doses from contact transfer are modelled.

As can be seen from the tables, in the Novozybkov example ^{131}I has the highest relative importance in connection with all dose contributions related to skin contamination. This is due to its large amount released, its high deposition velocity to skin and the generally short skin clearance half-life of the contaminants, which make the short radiological half-life of for instance ^{131}I somewhat less significant. For all skin contamination dose pathways in the Novozybkov case, the caesium isotopes (^{137}Cs and ^{134}Cs) give the second largest contribution. As increases in wind speed lead to increases in skin deposition velocity and indoor air concentrations will be smaller than those outdoor, the doses re-

ceived may well be greater than these estimates if the exposed persons are outdoor during the contaminant deposition phase.

6 Executive summary

Investigations made in the past have established that a relationship exists between the occurrence of some adverse health effects and the dermal deposition of airborne contaminants. In the radiological context, this contribution has, to date, been largely ignored in estimates of the total dose to exposed individuals. However, Jones has shown (Jones 1990, EUR 13013) that the predicted number of early deaths arising due to gamma and beta radiation doses is sensitive to the value used for aerosol deposition and residence time on skin. However, reliable aerosol deposition and clearance data for skin, hair and clothing are currently extremely limited. The present work aims to redress this by using sensitive tracer aerosol generation and detection techniques (employing both neutron activatable and fluorescent tracers) to study the deposition of airborne particles to skin, hair and clothing, and to investigate the retention and clearance of the deposited matter. The ultimate objective of the work is to develop models, based on experimental data as input, which can be used to estimate the doses potentially received from a direct contamination of humans.

An accurate estimation of the deposition velocity to skin - that is, the aerosol flux to the skin, divided by the ambient aerosol concentration- is underpinned by the ability to precisely measure the aerosol mass deposited on the body surface. In the present work, a variety of dermal exposure assessment techniques commonly used in the occupational environment were tested for suitability as tracer particle sampling technique, both in-vivo and in-vitro. Tests were carried out using neutron activatable and fluorescent particles (in the size range 0.5 microns to 8 microns) on in-vivo human skin and in-vitro post-operative human and rat skin. Qualitatively, skin wiping was found to be a satisfactory sampling technique for tracer aerosol particles, with good reproducibility and high integrity, borne out by the strong correlation between recovered tracer mass and wiped area. Quantitatively, wiping was found to remove of the order of 70% of the tracer aerosol from the skin.

Wiping, and other particle removal techniques, were also assessed in this work from the point of view of dermal decontamination efficacy, following an accidental radioactive aerosol exposure. Due to its high particle removal efficiency, wiping (and also tape-stripping) was considered to have some value as a dermal decontamination technique. However, analysis of repeated wipes on the same area of skin indicated that there exists a dislodgeable particle fraction. Furthermore, in-vitro experiments, where skin was exposed to fluorescent particles, wiped and then analysed by fluorescent microscopy, indicate that the wiping method enhances the degree of penetration to less accessible locations, such as hair follicles.

In addition to dedicated skin decontamination strategies which might be implemented following an accidental aerosol exposure, a fluorescence scanning system was developed so that the time course of decontamination on the skin during normal activities - everyday washing, or simple wearing-could be determined. Experiments with the scanning system indicated that cold water washing removed a substantial proportion of deposited 4.5 μm particles. Human activity experiments, whereby exposed individuals engaged in normal indoor and outdoor walking, yielded a clearance half life for 2.5 and 4.5 μm particles of the

order of respectively a few days and a few hours. This is significantly shorter than for instance the value used for all particle sizes in the accident consequence code COSYMA. However, it would be expected that the clearance half-life for sub-micron particles would be longer than that recorded for 2.5 μm particles. The clearance of sub-micron particles is likely to be governed by the shedding of the Stratum Corneum over a few weeks, although especially small particles may migrate to deeper skin crevices and hair follicles.

It is considered that a significant amount of information has been generated from the experimental work on skin sampling carried out under the contract, which not only has importance in the radiological context following an accident, but also in the occupational health context. A dermal exposure pathway, which is relevant to both contexts, is that of contact transfer between the skin and contaminated indoor surfaces. Experiments have been carried out to assess the significance of this pathway. The results indicate that a relatively large fraction of a thin layer of contaminants on a surface can be transferred to skin by contact. If the skin is damp, the transfer may be slightly greater.

Having developed a skin sampling protocol as outlined above, aerosol deposition velocity measurements on skin could be made, by exposing human volunteers to tracer aerosol in test chambers and in test rooms. The results indicated that the deposition velocities were in the range $0.4 \cdot 10^{-4}$ ms^{-1} - $192 \cdot 10^{-4}$ ms^{-1}, for particles in the size range 0.5 microns - 10 microns. These values were at least an order of magnitude higher than deposition velocities measured to inert building surfaces, both during the present measurements and as part of previous research, and for this reason, efforts were made to understand the underlying physics of aerosol interaction with the human body. The influence of the body's electrostatic potential on aerosol deposition was demonstrated by attaching an electrical grounding strap to one arm of a volunteer; this had the effect of reducing the deposition velocity of 4.5 μm particles by a factor of two. Air velocities measured in close proximity to the volunteer were found to be higher than ambient, suggesting that air turbulence, which promotes aerosol impaction, may arise due to the body's heat island. Measured aerosol deposition velocities on test surfaces attached to a volunteer and to a heated aluminium phantom indicated that surface roughness and electrostatic charge influenced aerosol deposition in the particle size range studied. A few experiments at elevated air velocities (2 $ms^{-1}$and 4 ms^{-1}) were carried out in a wind tunnel to measure aerosol deposition rates of 1 micron particles on a heated cylinder. These measurements showed that increasing wind speeds lead to increasing deposition velocity. This means that aerosol deposition on the body in the outdoor environment may be considerable.

In an accident situation, in addition to aerosol deposition to skin, doses also arise from aerosol interaction with hair and clothing. Due to the versatility of neutron activation analysis, sampling protocols for hair and clothing are relatively straightforward, since these materials, after an aerosol deposition interval, can be destructively analysed. Experiments were carried out to determine aerosol deposition velocities to hair and clothing, using both synthetic wigs and real human hair, and a range of synthetic and mixed-fibre clothing. Measured deposition velocities to hair were found to be of the same order of magnitude as those measured to skin, although much less dependent on particle size. A series of clothing washing experiments indicated a dependence of particle removal efficiency on particle size. Also, the data suggest that the micro-physical fibre structure (smooth in the case of synthetic fibres and rougher in the case of natural fibres) of clothing was a more important determinant of particle removal efficiency than the macro-physical weave of the garment itself. An experiment was carried out to determine clearance half-lives of particles from hair under

normal human activity. Here, a test person had a shower every morning, prior to each new exposure, and the clearance effect was found to be great, even though the particles applied were as small as 0.5 μm. For larger particles the effect is expected to increase.

To complement the experimental work, a computational model was developed for the calculation of doses from contamination of the human body after an airborne release of radioactive matter. Using measured aerosol concentrations for different isotopes in near-ground level air in Novozybkov, Russia, after the Chernobyl accident, size-specific indoor air concentrations were deduced using an empirical formula derived under a previous research contract. These were then multiplied by experimentally determined aerosol deposition velocities to skin to determine the total amount of radioisotope deposited on an area of skin, hair and clothing. Dose calculations were made on the basis of a simple Monte Carlo model for gamma emissions, with an ICRU sphere irradiated from the surface. The beta doses to skin were calculated from published data for an epidermis equivalent depth in water and at a depth corresponding to 0.4 mm thick clothing. In both cases, natural clearance from the skin, and radioactive decay of the isotopes, was taken into account. It was found that the largest dose contribution, both for gamma and beta emissions, came from ^{131}I, with other significant doses arising from ^{134}Cs and ^{137}Cs. The gamma doses were found to be in the same range as those received over the first year following the Chernobyl accident from contamination of outdoor surfaces by dry deposition of aerosol. Doses were also given in units relative to dry deposition of 1 MBq m^{-2} of the investigated isotopes to a reference surface (a cut grassed lawn). Also doses potentially received by skin contact transfer were evaluated.

7 Acknowledgements

The authors would like to acknowledge the Commission of the European Communities for support under the Nuclear Fission Safety RTD Programme, contract FI4PCT950019.

The support of NRPB in the UK for financing an extra PhD student at Imperial College is also acknowledged.

8 References

Andersson, K.G., 1996. Evaluation of Early Phase Nuclear Accident Clean-up Procedures for Nordic Residential Areas, NKS Report NKS/EKO-5(96)18, ISBN 87-550-2250-2.

Bell, KF (1994) An Investigation of the Effects of Heating and Air Movements on the Deposition of Aerosol to Body Surfaces. MSc dissertation, Imperial College of Science, Technology and Medicine, University of London, UK

Benzing, R, Parry, SJ, Baghini, NM and JA Davies (1993) Environmental and Personal Monitoring for Uranium by Delayed Neutron Counting. The Science of the Total Environment, Vol. 130/131, pp. 267-274.

Brouwer, D.H., Kroese, R., and J.J. Van Hemmen (1999) Transfer of contaminants from surfaces to hands: an experimental assessment of linearity of the exposure process, adherence to the skin, and area exposed during fixed pressure and repeated contact with surfaces contaminated with a powder. Appl. Occup. Environ. Hyg. (in press)

Byrne, M., Lange, C., Goddard, A.J.H. and J. Roed. Indoor Aerosol Deposition Measurements for Exposure Assessment Calculations. Proceedings of the 6th International Conference of Indoor Air Quality and Climate, Helsinki, Vol. 3, pp. 415-420, 1993.

Cross, W.G., Freedman, N.O. & Wong, P.Y., 1992. Beta ray dose distributions from skin contamination, Rad. Prot. Dosimetry vol. 40, no.3, pp. 149-168.

Dorrian, M.D., 1997. Particle size distributions of radioactive aerosols in the environment, Rad. Prot. Dosimetry vol. 69, no.2 pp. 117-132.

Faw, R.E., 1992. Absorbed doses to skin from radionuclide sources on the body surface, Health Phys. 63(4): 443-448.

Fenske, RA, Leffingwell JT and Spear RC (1986) A Video Imaging Technique for Assessing Dermal Exposure Instrument Design and Testing. American Industrial Hygiene Association Journal, Vol.47 No. 12, pp 764-770

Fogh, C.L.; Byrne, M.A.; Roed, J. and A.J.H. Goddard, Size Specific Indoor Aerosol Deposition Measurements and Derived I/O Concentration Ratios. Atmospheric Environment, Vol. 31, No. 15, pp. 2193-2203, 1997.

Grandolfo, M, Michaelson, SM and A Rindi (1985) Biological Effects and Dosimetry of Static and ELF Electromagnetic Fields. Plenum Press, New York.

Greason, WD (1994) Analysis of Human-Body Model for Electrostatic Discharge with Multiple Charged Sources. IEEE Transactions on Industry Applications. Vol. 30, No. 3, pp 589-594.

Gudmundsson, A, Schneider, T, Petersen, OH, Vinzents, PS, Bohgard, M and KR Akelsson (1992). Determination of particle deposition velocity onto the human eye. Journal of Aerosol Science, 23, S1, pp. 563-566.

Hodson, MJ, Smith RJ, van Blaaderen, A, Crafton T and O'Neill, CH (1994) Detecting Plant Silica Fibres in Animal Tissue by Confocal Fluorescence Microscopy. Annals of Occupational Hygiene, Vol. 38, No.2, pp. 149-160.

Homma, H. and M. Yakiyama, Examination of free Convection around Occupant's Body caused by its Metabolic Heat. ASHRAE Transactions, Vol. 94, Pr. 1, pp. 104-124, 1988.

ICRP Publication 23, 1974. Report of the task group on Reference Man, Pergamon Press.

ICRP publication 59, 1991. The biological basis for dose limitation in the skin, Pergamon Press, ISBN 0 08 041143 6.

ICRP Publication 60, 1990. 1990 Recommendations of the International Commission on Radiological Protection, Pergamon Press, ISBN 0 08 041144 4.

ICRU report 56, 1997. Dosimetry of External Beta Rays for Radiation Protection, International Commission on Radiation Units and Measurements,

7910 Woodmont Avenue, Bethesda, Maryland, USA, ISBN 0-913394-55-6.

Kinnersley, RP, Ould-dada Z and P James (1997) Production of Characterisation of Uranium Aerosols for use is Tracer Studies Employing Delayed Neutron Analysis. Submitted to Journal of Aerosol Science.

Kocher, D.C., 1980. Effects of indoor residence on radiation doses from routine releases of radionuclides to the atmosphere, Nuclear Technology, vol. 48, pp. 171-179.

Kryshev, I.I., 1996. Dose reconstruction for the areas of Russia affected by ^{131}I contamination, Rad. Prot Dosimetry vol. 64, no.1/2, pp. 93-96.

Lange, C., Indoor deposition and the protective effect of houses against airborne pollution, Risø report R-780(EN), Risø National Laboratory, ISBN 87-550-2024-0, 1995.

Nazaroff, WW and Cass, GR (1987) Particle deposition from a natural convection flow onto a vertical isothermal flat plate. Journal of Aerosol Science, 18, pp 445-455.

Ness, SA (1994) "Surface and Dermal Monitoring for Toxic Exposure". Published by Van Nostrand Reinhold

Parker, RC, Bull, RK, Stevens, DC and M Marshall (1990). Studies of aerosol distribution in a small laboratory containing a heated phantom. Annals of Occupational Hygiene, 34, No. 1, pp. 35-44.

Reineking, A., Becker, K.H., Porstendörfer, J. & Wicke, A., Air activity concentrations and particle size distributions of the Chernobyl aerosol, Rad. Prot. Dos. vol.19, no.3 pp. 159-163.

Roed, J., 1990. Deposition and removal of radioactive substances in an urban area, Final report of the project NKA AKTU-245, NKA, ISBN 87 7303 514 9.

Roed, J. & Cannell, R.J., 1987. Relationship between indoor and outdoor aerosol concentration following the Chernobyl accident, Rad. Prot. Dosimetry vol. 21, no. 1/3, pp. 107-110.

Roed, J.; Andersson, K. G.; Bell, K.F.; Byrne, M. A.; Fogh, C.L.; Goddard, A.J.H. and D.V. Vollmair, Quantitative Measurement of Aerosol Deposition on Skin, Hair and Clothing for Dosimetric Assessment, Risø-R-1028(EN), ISBN 87-550-2360-6, 1998.

Roff, MW (1994) A Novel Lighting System for the Measurement of Dermal Exposure Using a Fluorescent Dye and an Image Processor. Annals of Occupational Hygiene, Vol. 38, No. 6, pp. 903-919

Rohloff, F. & Heinzelmann, M. 1996. Dose rate by photon radiation to the basal layer of the epidermis in the case of skin contamination, Rad. Prot. Dosimetry vol. 63, no.1, pp. 15-28.

Rulik, P., Bucina, I. & Malatova, I., 1989. Aerosol particle size distribution in dependence on the type of radionuclide after the Chernobyl accident and in the NPP effluents, in proc. of the XVth regional congress of IRPA in Visby, Sweden, Sept. 1989.

Taylor, D.C., Hussein, E.M.A. & Yuen, P.S., 1997. Skin dose from radionuclide contamination on clothing, Health Phys. 72(6):835-841.

Thatcher, T.L. & Layton, D.W., 1995. Deposition, resuspension and penetration of particles within a residence, Atmospheric Environment vol. 29, No. 13, pp. 1487-1497.

9 Annexes

9.1 Skin wiping protocol

Similar, but independent, protocols have been developed at Risø and at Imperial College. It should however be emphasised that this presents no disparity in the determination of deposition velocities. It is not the case that one protocol is better than the other ; provided that both are well validated, either is applicable. Furthermore, in understanding the basis of dermal exposure assessment techniques, the existence of two somewhat different protocols is useful.

Imperial College

1. Skin is exposed to tracer particles
2. In another area, wipe samples are prepared by an unexposed individual., from cotton fabric. The area of the individual wipes is approximately 10 cm^2. Wipes are soaked in distilled water
3. Exposed individual is removed from the test environment, and gloved.
4. A template is placed on the arm of the exposed person and held in place by the unexposed individual. The template is made of rigid steel, with a circular hole of diameter 4 cm (within which the skin is wiped).
5. The unexposed individual blots excess moisture from the wipe, and conveys it, via forceps, to the gloved hand of the exposed individual, who wipes his own arm.
6. The used wipe is transferred to a clean labelled plastic bag.
7. Steps 6 and 7 are repeated 5 times.
8. All wipes are analysed together in the same plastic bag.

Risø protocol

1. Skin is exposed to tracer particles.
2. In another area, the wipe samples prepared by an unexposed individual., from Whatman 542 filter paper. The area of the individual wipes is approximately 8 cm2. The wipes are soaked in ethanol.
3. The exposed person is removed from the test environment
4. A template is placed on the arm of the exposed person and held in place by the unexposed individual. The template is made of flexible aluminium, with a rectangular hole of 8 cm2, within which the skin is wiped. The unexposed individual blots excess moisture from wipe, and rigorously wipes the arm of the volunteer.
5. The used wipe is transferred to a clean labelled plastic bag.
6. Steps 4 and 5 are repeated 3 times.
7. All wipes are separately analysed

Is has been found that despite differences in the sampling protocols, the removal efficiency of tracer is similar in both cases (quantitative wiping efficiencies were presented in the January 1997 report). Although cotton used at Imperial is more malleable than filter paper used at Risø as a wiping material, it is likely that ethanol, which may interact more effectively with grease on the skin that would distilled water, may be a more effective "wetting agent", so that the two techniques have comparable efficiency.

In both cases, measures were implemented which ensured that skin wiping was carried out in a rigorous and reproducible manner. At Risø , it was ensured that the same person always carried out the wiping, and this person was selected because he wiped in a particularly vigorous way. At Imperial College, it was feared that an element of restraint might be exercised in wiping the skin of another person, so that it was decided that the volunteers themselves would wipe their own skin. In the majority of cases (over 75%), the same volunteer was used.

9.2 The Imperial College Fluorescence Scanning System.

An alternative dermal exposure assessment technique to the use of neutron activatable aerosol tracers, and one which is completely non-invasive, is the use of aerosol labels in which fluorescence can be induced by appropriate illumination. The development of the Imperial College system for fluorescent labelling of aerosol particles and their subsequent illumination and detection, when deposited on skin, was proceeded by a literature review of previous work, as summarised below. Fluorescence scanning has been used extensively as a non-invasive technique for investigating many types of surface contamination: in agriculture, the efficiency of pesticide spraying has been assessed by adding a fluorescent dye to the pesticide mix (Evans et al, 1992) and using an intensified machine vision system to characterise the pattern of spray deposits on leaves. With reference to semiconductor fabrication, Opiolka et al (1994) studied particle contamination of flat surfaces by using a microscope to detect the light emitted by polystyrene microspheres labelled with a fluorescent dye. Also, in the context of radioactive dose assessment following nuclear accidents, Cannell et al (1987) used a video camera with an image intensifier to detect the light emitted by fluorescent dye-labelled particles, and a microcomputer to analyse the signal, in their investigation of the mechanical transport of particulate contamination into dwellings. Fluorescence scanning has been applied to the study of dermal contamination by several researchers. Fenske et al (1986), Bierman et al (1992), Archibald et al (1994) and Roff (1994) used ultra-violet fluorescence scanning systems, comprised of video cameras and microcomputers, to detect and quantify dermal exposure to chemicals such as pesticides. While most workers used plane banks of ultra- violet tubes to illuminate the subject and employed software algorithms to compensate for the curvature of the subject's surface, Roff (1994) used a dodecahedral arrangement of ultra-violet strip lights to provide uniform illumination of the subject's skin.

Most previous studies have addressed the issue of dermal contamination with fluorescent materials in highly-concentrated liquid forms; it was therefore possible to achieve strong fluorescent signals, so that interference from other sources, such as the skin itself, were not significant. The human skin is fluorescent under ultra-violet light (Anderson and Parrish 1982) and the level of skin auto-fluorescence may depend on the presence of dried skin or calluses (Vo-Dinh 1987) or the amount of previous exposure to sunlight. Since the antici-

pated fluorescence of tracer-labelled solid particles would be significantly less that that of liquids, the design of the Imperial College system included measures for avoidance of the interfering effects of skin auto-fluorescence. The main features of the Imperial College fluorescence scanning system are described below.

In a fluorescence scanning system, the tracer dye is induced to fluoresce by a excitation light source of a suitable wavelength. The emitted fluorescence is collected by a video camera and the analogue output is digitised by a frame grabber which is an input card connected to the computer. This input is a matrix of numbers which are proportional to the intensities of light collected by each pixel of the light-sensitive chip of the camera. Image processing software can then manipulate these numbers to deduce the quantity of tracer dye on the scanned surface. In order to minimise interference from skin auto-fluorescence, dyes that fluoresce strongly under visible light, rather than ultra-violet light, have been selected. The lighting used is high-power tungsten halogen white light, with the output filtered (by a Balzers Calflex 3000 heat mirror, combined with a Schott BG12 colour glass filter) to remove heat and give a monochromatic light at the excitation wavelength; the heat must be filtered out of the light output to give a constant operating temperature of 20 C for the excitation filter. The video camera purchased (Hitachi Denshi KPM1K monochrome) was chosen for maximum sensitivity to low light levels and has a filter (Schott OG515 colour glass filter) which blocks any reflected excitation light, thereby allowing only the fluorescent light into the camera. A fast computer (Dell Optiplex 560L), with a frame grabber (Matrox Comet), gives maximum speed of image processing. The image processing software used was Matrox Hi-Tools. The test aerosols used to date are monodisperse silica particles. The tracer dye, fluorescent isothiocyanate, may be attached to the silica particles by a method developed by Hodson et al (1994) to attach tracer dyes to plant silica fibres. The system described above has been tested for its ability to detect tracer-labelled particles, when deposited both on filter paper and on human skin. The tests indicate that the sensitivity of detection is significantly lower than neutron activation analysis, so that higher surface loadings of particles will be required for accurate quantitative analysis of fluorescent aerosol.

References for section 9.2

Anderson R.R. and Parrish. J.A. In-Vivo Fluorescence of Human Skin: Woods Lamp. In: Optical Properties of Human Skin in The Science of Photomedicine. ed Regan J.D. and Parrish J.A. pp. 179-180. Plenum Press

Archibald B.A., Solomon K.R. and Stephenson G.R. 1994. A New Method for Calibrating the Video Imaging Technique for Assessing Dermal Exposure to Pesticides. Archives of Environmental Contamination and Toxicology. Vol. 26, pp. 398-402.

Bierman E.P.B., Brouwer D.H. and van Hemmen J.J. 1992. Quantification of Dermal Exposure with an Image Analysis System: Instrumental Design. [Abs] International Occupational Hygiene Association, First International Scientific Conference, Brussels, Belgium. December.

Bühler U. and Wienert V., 1993. Möglichkeiten und Grenzen der Dermofluorographie. Perfusion. Vol. 6, No. 6, pp. 246-252. Cannell R.J., Goddard A.J.H. and ApSimon H.M., 1987. Contamination of Dwellings by Particulate Matter: Ingress and Distribution Within the Dwelling. Radiation Protection Dosimetry, Vol. 21, No. 1/3, pp. 111-116.

Evans M.D., Law S.E. and Cooper S.C., 1992. Image Analysis of Particulate Spray Deposits Using Light Intensified Machine Vision. Proceedings of

the Meeting of American Society of Agricultural Engineers in Charlotte, N.C. Paper No. 927015.

Hodson M.J., Smith R.J., van Blaaderen A., Crafton T. and O'Neill C.H., 1994. Detecting Plant Silica Fibres in Animal Tissue by Confocal Fluorescence Microscopy. Annals of Occupational Hygiene. Vol. 38, No. 2, pp. 149-160.

Opiulka S., Schmidt F. and Fissan H., 1994. Combined Effects of Electrophoresis and Thermophoresis on Particle Deposition onto Flat Surfaces. Journal of Aerosol Science. Vol. 25, No.4, pp. 665-671.

Evans M.D., Law S.E. and Cooper S.C., 1992. "Image analysis of Particulate Spray Deposits Using Light Intensified Machine Vision". Proceedings of the Meeting of American Society of Agricultural Engineers in Charlotte, N.C. Paper No 927015.

Fenske R.A., Leffingwell J.T., and Spear R.C., 1986. "A Video Imaging Technique for Assessing Dermal Exposure I. Instrument Design and Testing. "American Industrial Hygiene Association Journal. Vol. 47(12) : pp. 764-770

Roff M.W., 1994. "A Novel Lighting System for the Measurement of Dermal Exposure Using a Fluorescent Dye and an Image Processor." Annals of Occupational Hygiene. Vol. 38, No. 6, pp. 903-919

Vo-Dinh T., 1987. "Evaluation of an Improved Fibre optics Luminescence Skin Monitor with Background Correction." American Industrial Hygiene Association Journal. Vol. 48(6) : pp. 594-598

Bibliographic Data Sheet **Risø-R-1075(EN)**

Title and authors

Quantitative measurement of aerosol deposition on skin, hair and clothing for dosimetric assessment - final report

C.L. Fogh, M.A. Byrne, K.G. Andersson, K.F. Bell, J. Roed, A.J.H. Goddard, D.V. Vollmair and S.A.M. Hotchkiss.

ISBN	ISSN
87-550-2360-6	0106-2840

Department or group	Date
Nuclear Safety Research and Facilities Department	03-06-99

Groups own reg. number(s)	Project/contract No(s)
	FI4PCT950019

Pages	Tables	Illustrations	References
58	20	22	46

Abstract (max. 2000 characters)

In the past, very little thought has been given to the processes and implications of deposition of potentially hazardous aerosol directly onto humans. This state of unpreparedness is unsatisfactory and suitable protocols have been developed and validated for tracer experiments to investigate the deposition and subsequent fate of contaminant aerosol on skin, hair and clothing. The main technique applied involves the release and subsequent deposition on volunteers in test rooms of particles of different sizes labelled with neutron activatable rare earth tracers. Experiments indicate that the deposition velocity to skin increases linearly with the particle size. A wind tunnel experiment simulating outdoor conditions showed a dependence on skin deposition velocity of wind speed, indicating that outdoor deposition velocities may be great. Both *in vivo* and *in vitro* experiments were conducted, and the influence of various factors, such as surface type, air flow, heating and electrostatics were examined. The dynamics of particle removal from human skin were studied by fluorescence scanning. This technique was also applied to estimate the fraction of aerosol dust transferred to skin by contact with a contaminated surface. The various parameters determined were applied to establish a model for calculation of radiation doses received from deposition of airborne radioactive aerosol on human body surfaces. It was found that the gamma doses from deposition on skin may be expected to be of the same order of magnitude as the gamma doses received over the first year from contamination on outdoor surfaces. According to the calculations, beta doses from skin deposition to individuals in areas of Russia, where dry deposition of Chernobyl fallout led to very high levels of contamination, may have amounted to several Sievert and may thus be responsible for a significant cancer risk.

Descriptors INIS/EDB

AEROSOLS; DEPOSITION; DYSPROSIUM 165; INDIUM 115; INDOOR AIR POLLUTION; PARTICLE SIZE; SAMPLING; SKIN; HAIR; CLOTHING; TRACER TECHNIQUES; CLEARANCE; FLUORESCENCE SCANNING; DOSES

Available on request from Information Service Department, Risø National Laboratory,
(Afdelingen for Informationsservice, Forskningscenter Risø), P.O.Box 49, DK-4000 Roskilde, Denmark.
Telephone +45 46 77 40 04, Telefax +45 46 77 40 13